Decoherence in a system of strongly coupled quantum oscillators. I. Symmetric network

M. A. de Ponte,* M. C. de Oliveira,† and M. H. Y. Moussa‡
Departamento de Física, CCET, Universidade Federal de São Carlos, Via Washington Luiz Km 235, São Carlos, 13565-905, SP, Brazil
(Received 6 January 2004; published 30 August 2004)

In this work we analyze the coherence dynamics and estimate decoherence times of quantum states in a network composed of N coupled dissipative quantum oscillators. We assume a symmetric network where all oscillators are coupled to each other with the same coupling strength. Master equations are derived for regimes of both weak and strong coupling between the oscillators. The strong coupling regime is characterized by the coupling strength between the oscillators or by the number of oscillators in the network. The decoherence times of particular states of the network are computed and the results are clarified by analyzing the processes of state swap and recurrence of reduced states of the network together with the linear entropies of the joint and reduced systems.

DOI: 10.1103/PhysRevA.70.022324 PACS number(s): 03.67.−a, 03.65.Ud, 03.65.Yz

I. INTRODUCTION

Since the discovery by Shor [1] that quantum information processing provides a means of integer factorization much more efficient than conventional computation, the subject of quantum networks has attracted considerable attention in the literature. Shor's contribution extracted a variety of quantum phenomena from their original purely theoretical context in the foundations of quantum mechanics and revealed the possibility of using them to inaugurate a novel technology for quantum communication [2] and computation [3]. Besides the striking character of quantum-state superpositions, which contain a major ingredient of a quantum logic processor—quantum bits—entanglement and nonlocality also play key roles in the emerging scenario of quantum information. The interference phenomenon characteristic of quantum superposition states allows parallel computation paths which can reinforce or cancel one another, depending on their relative phase [4]. In a quantum processor, entanglement and nonlocality are not only indispensable for correlating the input qubits in quantum gates, but also strikingly different from any classical operation: states can be transmitted from one node of a network to another by quantum teleportation [5,6].

As superpositions and entanglements of quantum states comprise the main ingredients for quantum information processing, another fundamental quantum phenomenon, the decoherence process [7–9], acts to destroy the quantum bits and their correlation altogether. It is generally accepted that decoherence is the main remaining obstacle to the processing of mass information. As decoherence stems from the inevitable coupling of quantum systems to their reservoirs, as well as from fluctuations arising in the very interactions required to manipulate quantum information, it is extremely difficult to deal with this phenomenon. However, exciting ideas have been pursued to make possible some degree of control over the decoherence of superposition states. The problem of finding efficient quantum-error-correction codes, similar to those of classical information-processing, is a major challenge in present-day quantum information theory [10]. Moreover, proposals for quantum-reservoir engineering have been put forward, in which additional interactions with the system of interest are engineered in order to weaken the inevitable coupling with its surroundings. The quantum-reservoir engineering program has attracted attention especially in the domain of trapped ions [11–13] and, specifically, a scheme has been presented for engineering squeezed-bath-type interactions to protect a two-level system against decoherence [14].

Parallel to the recent remarkable experimental realization of Shor's quantum factoring algorithm using nuclear magnetic resonance [15], interest has grown over the last few years in the coherence dynamics in a quantum network. For a simple network of two coupled systems, a theoretical model [16] has been provided for an earlier experimental proposal [17], where the coupling of the resonators to their environments is taken into account when the reversibility of coherence loss is analyzed. A system of two coupled cavities has also been analyzed [18], in which just one of the cavities interacts with a reservoir; a master equation is derived for the case of strongly coupled cavities and it is shown that the relaxation term is not simply the standard one, obtained by neglecting the interaction between the cavities. The present authors have analyzed the reversible decoherence process [19], as in the earlier works [16,17], but considering also the regime of strongly-coupled cavities, as in Ref. [18], and some remarkable coherence properties appeared. A method for modeling decoherence in an N-dimensional quantum system coupled to an N^2-dimensional quantum environment was recently presented [20].

As a step towards more realistic quantum-information processors, we are concerned in the present work with the phenomena of nonlocality and decoherence in the context of a network of N interacting dissipative oscillators, considering a symmetric network where each oscillator interacts with the other as sketched in Fig. 1. A different topology, which we call a central-oscillator network, is analyzed in the second part of this work, where a central oscillator is assumed to interact with the remaining $N-1$ noninteracting oscillators. Evidently, in the case of a symmetric network any oscillator

*Electronic address: maponte@df.ufscar.br
†Electronic address: marcos@df.ufscar.br
‡Electronic address: miled@df.ufscar.br

 ©2004 The American Physical Society

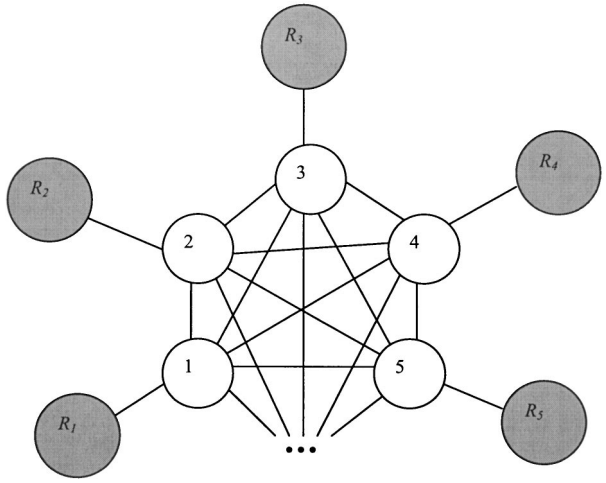

FIG. 1. Sketch of a symmetric network where each oscillator ($m=1,2,\ldots,N$) interacts with each other and its respective reservoir R_m.

can be picked out while in the case where a central oscillator is assumed, we focus exactly on this oscillator. In both topologies we are concerned with the coherence dynamics and the decoherence of the joint quantum states of the whole network and reduced states of particular oscillators. Specifically, we analyze the decoherence process, focusing on a single oscillator which, apart from interacting with its respective reservoir, also interacts with the remaining $N-1$ coupled oscillators plus their reservoirs. Considering all oscillators to have the same natural frequency ω_0 and all couplings the same strength λ, in Sec II master equations are derived for both weak ($\lambda \ll \omega_0$) and strong ($\lambda \approx \omega_0$) coupling regimes. (Below the definition of weak and strong coupling regime will be extended.)

II. A SYMMETRIC NETWORK

Starting with the symmetric network, we assume that the interactions between the oscillators, as well as between each oscillator and its reservoir, are described by the rotating wave approximation. Since the strong-coupling limit will be analyzed, a positive-definite Hamiltonian is assumed so that the energy spectrum has a lower bound [21,22]. Assuming, from here on, that the subscripts m and n, labeling the oscillators of the network, run from 1 to N, the system Hamiltonian is given by ($\hbar=1$)

$$H = \sum_{m,n(m\neq n)} \frac{\omega_0}{N-1}\left(a_m^\dagger + (N-1)\frac{\lambda}{2\omega_0}a_n^\dagger\right)\left(a_m + (N-1)\frac{\lambda}{2\omega_0}a_n\right) + \sum_{m,k}\omega_{mk}\left(b_{mk}^\dagger + \frac{V_{mk}}{\omega_{mk}}a_m^\dagger\right)\left(b_{mk} + \frac{V_{mk}}{\omega_{mk}}a_m\right), \tag{1}$$

where $a_m^\dagger$ and a_m are, respectively, the creation and annihilation operators for the oscillators whereas b_{mk} and $b_{mk}^\dagger$ are the analogous operators for the kth bath oscillator of system m, whose corresponding frequency and coupling strength are ω_{mk} and V_{mk}, respectively. Assuming that the coupling between the oscillators and their reservoirs satisfies the condition $\Sigma_k (V_{mk})^2/\omega_{mk} \ll \omega_0$, we obtain from Eq. (1) the Hamiltonian $H=H_0^S+H_0^R+V$, given by

$$H_0^S = \tilde{\omega}_0\sum_m a_m^\dagger a_m + \frac{\lambda}{2}\sum_{m,n(m\neq n)}(a_m^\dagger a_n + a_m a_n^\dagger), \tag{2a}$$

$$H_0^R = \sum_{m,k}\omega_{mk}b_{mk}^\dagger b_{mk}, \tag{2b}$$

$$V = \sum_{m,k} V_{mk}(a_m^\dagger b_{mk} + a_m b_{mk}^\dagger), \tag{2c}$$

where $\tilde{\omega}_0$ is related to the natural frequency ω_0 as follows:

$$\tilde{\omega}_0 = \omega_0\left[1 + (N-1)^2\frac{\lambda^2}{(2\omega_0)^2}\right]. \tag{3}$$

We note from Eq. (3) that even in the weak-coupling limit ($\lambda/\omega_0 \ll 1$) the natural frequency will be appreciably shifted when $\lambda/(2\omega_0) \gtrsim 1/(N-1)$. Therefore, whenever $\lambda/(2\omega_0) \gtrsim 1/(N-1)$ we have to start from a positive-definite Hamiltonian given by Eq. (1). Note that since we are assuming weak coupling between the systems and their reservoirs, it is unnecessary to write these interactions in a positive-definite form as in Eq. (1). However, the positive-definite form employed for the coupling between the systems ensures an energy spectrum with a lower bound, whatever the value of the coupling strength λ. The Hamiltonian H_0^S can be diagonalized through the canonical transformation

$$A_1 = \frac{1}{\sqrt{N}}\sum_n a_n, \tag{4a}$$

$$A_\ell = \frac{1}{\sqrt{\ell(\ell-1)}}\left[\sum_{j=1}^{\ell-1} a_j - (\ell-1)a_\ell\right], \tag{4b}$$

where, from here on, $\ell=2,3,\ldots,N$ and the operator A_m satisfies the same commutation relation as a_m: $[A_m,A_n]=0$ and $[A_m,A_n^\dagger]=\delta_{mn}$. The aim of these new operators is to decouple the direct interactions between the oscillators, coming from the second term on the right hand side of Eq. (2a). Consequently, indirect interactions between the oscillators will be created through their respective reservoirs, as described by Hamiltonian $\mathbf{H}=\mathbf{H}_0+\mathbf{H}_I$, with

$$\mathbf{H}_0 = \sum_m\left(\Omega_m A_m^\dagger A_m + \sum_k \omega_{mk}b_{mk}^\dagger b_{mk}\right), \tag{5a}$$

$$\mathbf{H}_I = \sum_{m,n,k} C_{mn}V_{nk}(A_m^\dagger b_{nk} + A_m b_{nk}^\dagger). \tag{5b}$$

The shifted frequencies, corresponding to the normal modes of the coupled systems, are given by

$$\Omega_1 = \tilde{\omega}_0 + (N-1)\lambda, \tag{6a}$$

$$\Omega_\ell = \tilde{\omega}_0 - \lambda, \tag{6b}$$

while the coefficient C_{mn} satisfies the relations $C_{1n}=1/\sqrt{N}$, $C_{\ell 1}=1/\sqrt{\ell(\ell-1)}$, $C_{\ell\ell}=-\sqrt{(\ell-1)/\ell}$, $C_{\ell\ell'}=0$ for $\ell<\ell'$, and $C_{\ell\ell'}=1/\sqrt{\ell(\ell-1)}$ for $\ell'<\ell<N$. As with ℓ, we assume that $\ell'=2,\ldots,N$. It is clear from Hamiltonian (5b) that the new operators A_m represent uncoupled oscillators which interact, however, with all reservoirs. Without the direct coupling between the oscillators, as modelled by Hamiltonian **H**, it becomes simpler to derive the equation for the evolution of the density matrix of the N coupled oscillators, $\rho_{1,\ldots,N}(t)$, in the interaction picture, to the second order of perturbation

$$\frac{d\rho_{1,\ldots,N}(t)}{dt} = -\frac{1}{\hbar^2}\int_0^t dt' \mathrm{Tr}_R[\mathbf{V}(t),[\mathbf{V}(t'),\rho_R(0)\otimes\rho_{1,\ldots,N}(t)]], \tag{7}$$

where $\mathbf{V}(t)=\exp(i\mathbf{H}_0 t/\hbar)\mathbf{H}_I \exp(-i\mathbf{H}_0 t/\hbar)$. Defining the reservoir operators $\mathcal{O}^\dagger_{mn}(t)=\Sigma_k V_{nk} b^\dagger_{nk}\exp[i(\omega_{nk}-\Omega_m)t]$, we obtain $\mathbf{V}(t)=\Sigma_{m,n} C_{mn}(A^\dagger_m \mathcal{O}_{mn}+A_m\mathcal{O}^\dagger_{mn})$. We have to solve the integrals appearing in Eq. (7), related to correlation functions of the form

$$\int_0^t dt'\langle \mathcal{O}_{mn}(t)\mathcal{O}^\dagger_{m'n}(t')\rangle = \sum_{k,k'}\int_0^t dt' V_{nk}V_{nk'}\langle b_{nk}b^\dagger_{nk'}\rangle \times\exp[-i(\omega_{nk}-\Omega_m)t + i(\omega_{nk'}-\Omega_{m'})t'], \tag{8}$$

where, as with m and n, we assume henceforward that m' and n' run from 1 to N. Assuming that the reservoir frequencies are very closely spaced to allow a continuum summation and remembering that the function $\mathrm{N}_n(\omega_{nk})$ is defined by

$$\langle b^\dagger_n(\omega_{nk})b_n(\omega_{nk'})\rangle = 2\pi \mathrm{N}_n(\omega_{nk})\delta(\omega_{nk}-\omega_{nk'}), \tag{9}$$

we obtain

$$\begin{aligned}\int_0^t dt'\langle \mathcal{O}_{mn}(t)\mathcal{O}^\dagger_{m'n}(t')\rangle &= \int_0^t dt'\int_0^\infty \frac{d\omega_{nk}}{2\pi}\int_0^\infty \frac{d\omega_{nk'}}{2\pi}\sigma_n(\omega_{nk})\sigma_n(\omega_{nk'})V_{nk}(\omega_{nk}) \\ &\times V_{nk'}(\omega_{nk'})[\mathrm{N}_n(\omega_{nk})+1]2\pi\delta(\omega_{nk}-\omega_{nk'}) \\ &\times\exp[-i(\omega_{nk}-\Omega_m)t + i(\omega_{nk'}-\Omega_{m'})t'] \\ &= \exp[i(\Omega_m-\Omega_{m'})t]\int_0^t dt'\int_0^\infty \frac{d\omega_{nk}}{2\pi} \\ &\times[\sigma_n(\omega_{nk})V_{nk}(\omega_{nk})]^2[\mathrm{N}_n(\omega_{nk})+1] \\ &\times\exp[-i(\omega_{nk}-\Omega_{m'})(t-t')],\end{aligned} \tag{10}$$

$\sigma_n(\omega_{nk})$ being the density of states of reservoir n. Performing the variable transformations $\tau=t-t'$ and $\varepsilon=\omega_{nk}-\Omega_{m'}$ we obtain

$$\begin{aligned}\int_0^t dt'\langle \mathcal{O}_{mn}(t)\mathcal{O}^\dagger_{m'n}(t')\rangle &= \exp[i(\Omega_m-\Omega_{m'})t]\int_{-\Omega_{m'}}^\infty \frac{d\varepsilon}{2\pi}[\sigma_n(\varepsilon+\Omega_{m'})V_{nk}(\varepsilon+\Omega_{m'})]^2[\mathrm{N}_n(\varepsilon+\Omega_{m'})+1]\int_0^t d\tau e^{-i\varepsilon\tau}.\end{aligned} \tag{11}$$

We note that the minimum normal mode frequency Ω_ℓ is given by $\Omega_\ell|_{\min}=\omega_0 N(N-2)/(N-1)^2$, a value which follows from $\lambda=2\omega_0/(N-1)^2$. Therefore, when $N\gg 1$, $\Omega_\ell|_{\min}\approx\omega_0$. In the particular case where $N=2$, we obtain $\lambda=2\omega_0$, such that $\Omega_\ell|_{\min}\approx 0$, as discussed in Ref. [19]. In what follows, considering the general case of N coupled oscillators, we will be interested in the coupling strength $\lambda=2\omega_0$ such that $\Omega_\ell=N(N-2)\omega_0$ and $\Omega_1=N^2\omega_0$, i.e., with $N\gg 1$, both normal modes around $N^2\omega_0$ are shifted to regions far from the oscillators' natural frequency ω_0.

As usual when deriving the master equation, we assume that $V_{nk}(\varepsilon+\Omega_m)$, $\sigma_n(\varepsilon+\Omega_m)$, and $\mathrm{N}_n(\varepsilon+\Omega_m)$ are functions that vary slowly around the frequency Ω_m. Observing that the last integral in Eq. (11) contributes significantly only when $|\varepsilon t|\lesssim 1$, so that we extend the upper limit of the time integration to infinity, the expression for the correlation function becomes

$$\int_0^t dt'\langle \mathcal{O}_{mn}(t)\mathcal{O}^\dagger_{m'n}(t')\rangle = \frac{N}{2}\gamma_n(\Omega_{m'})[\mathrm{N}_n(\Omega_{m'})+1] \times\exp[i(\Omega_m-\Omega_{m'})t], \tag{12}$$

where the damping rates are defined as

$$\gamma_n(\Omega_m) = \frac{1}{N}V^2_{nk}(\Omega_m)\sigma^2_n(\Omega_m)\int_{-\Omega_m}^\infty d\varepsilon\,\delta(\varepsilon). \tag{13}$$

For $N=2$ and $\lambda=2\omega_0$, such that $\Omega_1=4\omega_0$ and $\Omega_2|_{\min}\approx 0$, we obtain

$$\gamma_n(\Omega_1) = \tfrac{1}{2}V^2_{nk}(\Omega_1)\sigma^2_n(\Omega_1), \tag{14a}$$

$$\gamma_n(\Omega_2|_{\min}) = \tfrac{1}{4}V^2_{nk}(\Omega_2|_{\min})\sigma^2_n(\Omega_2|_{\min}). \tag{14b}$$

For $N>2$ and any value of λ, we obtain

$$\gamma_n(\Omega_m) = \frac{1}{N}V^2_{nk}(\Omega_m)\sigma^2_n(\Omega_m). \tag{15}$$

Defining the damping rate $\Gamma_n\equiv V^2_{nk}(\omega_0)\sigma^2_n(\omega_0)$, we obtain from Eq. (13), in the weak-coupling regime, the result

$$\gamma_n(\omega_0) = \frac{1}{N}V^2_{nk}(\omega_0)\sigma^2_n(\omega_0) = \frac{\Gamma_n}{N}. \tag{16}$$

III. THE MASTER EQUATION

Defining the simplified expressions $\gamma_n(\Omega_1)=\gamma^+_n$, $\mathrm{N}_n(\Omega_1)=\mathrm{N}^+_n$, $\gamma_n(\Omega_\ell)=\gamma^-_n$, $\mathrm{N}_n(\Omega_\ell)=\mathrm{N}^-_n$ and using Eqs. (4a) and (4b) along with the coefficients C_{mn} defined above, we obtain the master equation in the Schrödinger picture

$$\frac{d\rho_{1,\ldots,N}(t)}{dt} = i\Bigg[\rho_{1,\ldots,N}(t), \tilde{\omega}_0 \sum_m a_m^\dagger a_m + \frac{\lambda}{2}\sum_{m,n(m\neq n)}(a_m^\dagger a_n + a_m a_n^\dagger)\Bigg] + \sum_m \mathcal{L}_m \rho_{1,\ldots,N}(t) + \sum_{m,n(m\neq n)} \mathcal{L}_{mn}\rho_{1,\ldots,N}(t), \tag{17}$$

where the Liouville operators $\mathcal{L}_m\rho_{1,\ldots,N}(t)$ are given by

$$\mathcal{L}_m\rho_{1,\ldots,N}(t) = \tfrac{1}{2}\{[\gamma_m^+ + (N-1)\gamma_m^-]([a_m\rho_{1,\ldots,N}(t), a_m^\dagger] + [a_m, \rho_{1,\ldots,N}(t)a_m^\dagger]) + [\gamma_m^+ \mathrm{N}_+^m + (N-1)\gamma_m^- \mathrm{N}_-^m] \times ([[a_m, \rho_{1,\ldots,N}(t)], a_m^\dagger] + [[a_m^\dagger, \rho_{1,\ldots,N}(t)], a_m])\}, \tag{18}$$

and those for the cross-decay channels by

$$\mathcal{L}_{mn}\rho_{1,\ldots N}(t) = \tfrac{1}{2}((\gamma_m^+ - \gamma_m^-)\{[a_n\rho_{1,\ldots,N}(t), a_m^\dagger] + [a_m, \rho_{1,\ldots,N}(t)a_n^\dagger]\} + (\gamma_m^+ \mathrm{N}_m^+ - \gamma_m^- \mathrm{N}_m^-) \times \{[[a_n, \rho_{1,\ldots,N}(t)], a_m^\dagger] + [[a_n^\dagger, \rho_{1,\ldots,N}(t)], a_m]\}). \tag{19}$$

The master equation (17) is a general form valid for the strong-coupling regime. Evidently, the cross-decay channels $\mathcal{L}_{mn}\rho_{1,\ldots,N}(t)$, given the strong coupling between the systems, can be of the same order of magnitude as the direct-decay channels $\mathcal{L}_m\rho_{1,\ldots,N}(t)$. In the weak-coupling regime, where $\gamma_m^\pm \approx \Gamma_m/N$ [see Eq. (16)] and $\mathrm{N}_m^\pm \approx \mathrm{N}_m$ (see discussion below), the cross-decay channels cancel out and the master equation (17) reduces to the expected form for N independent dissipative oscillator, where the Liouville operators simplify to the well-known structure

$$\mathcal{L}'_m\rho_{1,\ldots,N}(t) = \tfrac{1}{2}\Gamma_m\{([a_m\rho_{1,\ldots,N}(t), a_m^\dagger] + [a_m, \rho_{1,\ldots,N}(t)a_m^\dagger]) + \mathrm{N}_m([[a_m, \rho_{1,\ldots,N}(t)], a_m^\dagger] + [[a_m^\dagger, \rho_{1,\ldots,N}(t)], a_m])\}. \tag{20}$$

We stress that for a network with a large number of oscillators, the normal modes Ω_1 and Ω_ℓ, depending on the factor $N-1$, can be shifted to regions far from the natural frequency ω_0, even for small values of the coupling strength λ. This is a central feature of a network with $N \gg 1$, since in this case we have always to consider the cross-decay channels, which emerge due to unequal values for the damping rates γ_n^- and γ_n^+. From this observation we conclude that in a realistic quantum logical processor, the number of dissipative nodes will always be a matter for concern—when analyzing the coherence dynamics and decoherence times—even in the case of weak coupling between these nodes.

Splitting the damping rate

A central point to be noted, when deriving the master equation for the strong coupling regime, is that the damping rate for each oscillator γ_m splits into two different values, γ_m^+ and γ_m^-. To illustrate this mechanism, which is due to the splitting of the shifted frequency $\tilde{\omega}_0$ into the normal modes

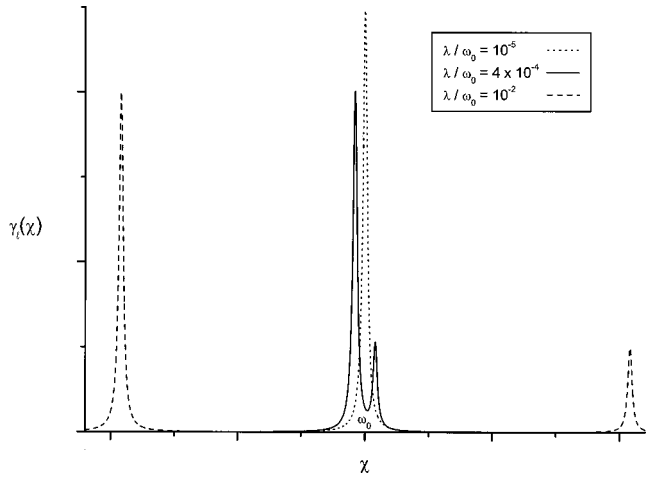

FIG. 2. Damping function $\Gamma_m(\chi)$, assuming Lorentzian coupling V_{mk} between oscillator m and its respective reservoir. In the weak-coupling regime the function $\Gamma_m(\chi)$ is centered around ω_0 (dotted line). As λ increases, the damping function splits into two Lorentzian functions whose peak heights are $1/N$ and $(N-1)/N$ times the original value $\Gamma_m(\omega_0)$ (solid line), where N is the number of oscillators. In this figure we plot $\Gamma_m(\chi)$ for a five-oscillator network.

Ω_1 and Ω_ℓ, we assume a Lorentzian coupling V_{mk} between the systems and their respective reservoirs, such that the damping function $\Gamma_m(\chi)$, centered on frequency χ_0, is given by

$$\Gamma_m(\chi) = \sigma_m^2 \frac{\varkappa}{(\chi-\chi_0)^2 + \varkappa^2}, \tag{21}$$

with the parameter $\varkappa$ specifying for the spectral sharpness around the mode frequency. From the above expression and remembering that the shifted frequency $\tilde{\omega}_0$ splits into two distinct values Ω_1 and Ω_ℓ, we obtain the Lorentzian damping function depicted in Fig. 2 (for $N=5$):

$$\Gamma_m(\chi) = \frac{\varkappa\sigma_m^2}{N}\left(\frac{1}{(\chi-\Omega_1)^2+\varkappa^2} + \sum_\ell \frac{1}{(\chi-\Omega_\ell)^2+\varkappa^2}\right) = \gamma_m(\Omega_1) + \sum_\ell \gamma_m(\Omega_\ell), \tag{22}$$

with maxima at Ω_1 and Ω_ℓ. We observe that in the weak-coupling regime, when $\Omega_1 = \Omega_\ell \approx \omega_0$, such that $\gamma_m(\omega_0) + \Sigma_\ell\, \gamma_m(\omega_0) = \Gamma_m$ [see Eq. (16)], we obtain from the general Liouville operator (18), the usual Liouville form for N independent dissipative oscillators (20). Moreover, it is immediately obvious from Eq. (22) that in the weak-coupling regime, where $\Omega_m \approx \omega_0$, the damping function has only one peak, shown by the dotted line in Fig. 2. In this regime, the damping rate, assumed to be the maximum of a sharp-peaked damping function, i.e., $\Gamma_m(\omega_0) = \Gamma_m$ (for a small value of $\varkappa$), becomes N times higher than the value designated for $\gamma_m(\Omega_1)$ and $\gamma_m(\Omega_\ell)$. However, as λ increases, the damping function splits into two Lorentzian functions whose peak heights are smaller than the original value Γ_m, as dictated by the master equation (17) and shown by the solid line in Fig. 2. The dashed line shows the situation where the two peaks

can clearly be distinguished, on the way to the strong-coupling regime, $\lambda/\omega_0 \approx 1$. For $N \gg 1$ both peaks, centered on Ω_1 and Ω_ℓ, shift to around the value $N^2\omega_0$ and can hardly be distinguished. In practice, the effect of the strong coupling between the systems is essentially to shift the normal-mode frequencies Ω_1 and Ω_ℓ to regions far from the natural system frequency ω_0. Therefore, if the spectral densities of the reservoirs around the normal-mode frequencies are significantly different from that around ω_0, the coherence dynamics of the system may be significantly modified. Thus, the spectral densities of the reservoirs play a crucial role in the dissipative dynamics of strongly-coupled systems, since the magnitude of the damping rate γ_m depends on σ_m. For this reason, in the next section we analyze different spectral densities of the reservoirs in order to illustrate the interesting features arising from the stron-coupling regime.

Finally, we note that the splitting of the Lorentzian in Eq. (21) into those in Eq. (22) becomes more pronounced as λ and/or N increase. As explained above, the existence of a large number of oscillators in the network also shifts the normal modes to regions far from the natural frequency ω_0. In other words, we have to increase the parameter $\lambda(N-1)$, through the coupling strength and/or the number of oscillators in the network, to enable us to explore different regions of the spectral density of the reservoir. From this perspective, from here on we refer to the coupling as strong when the parameter $\lambda(N-1)$ is sufficiently large for the cross-decay channels to have to be taken into account.

IV. SPECTRAL DENSITIES OF THE RESERVOIRS

Evidently, the spectral densities of the reservoirs depend on the nature of the coupled dissipative oscillators under study. Considering, for example, surface electrons trapped in harmonic potentials over liquid helium [23], the reservoirs become essentially the bulk phonons of the liquid helium. For such a phonon reservoir, the Debye model, where $\sigma_m(\Omega_{1,\ell}) \sim \Omega_{1,\ell}^2$, applies very well for the domain of small frequencies, whereas the spectral densities go to zero for the high-frequency domain. In this case a Lorentzian function can safely be used to model the spectral densities of the reservoirs.

Apart from the physical nature of the dissipative oscillators, specific spectral densities could be achieved through engineered reservoirs, a program which has recently attracted considerable attention for controlling the decoherence process of quantum states [11–14]. Therefore, the results we present below, depending crucially on the spectral density of the reservoir, might provide a motivation for future theoretical proposals on engineered reservoirs. For the following discussion we consider the strong coupling regime and set the reservoir temperatures to zero, remembering, from definitions $\gamma_n(\Omega_1) = \gamma_n^+$ and $\gamma_n(\Omega_\ell) = \gamma_n^-$, that the parameter $\gamma_n^\pm$ accounts for the intensity of the system-reservoir interaction around Ω_m, i.e., $\gamma_n^\pm$ depends on the reservoir spectral density around the normal-mode frequencies.

A. Markovian white noise

We start with the simplest model of Markovian white noise, where the spectral density of the reservoir is invariant over translation in frequency space, as depicted in Fig. 3(a). In this case, assuming a Lorentzian coupling between the oscillators and their respective reservoirs, centered around the normal-mode frequencies, as in Eq. (22), we get exactly the same result as in the weak coupling regime $\gamma_m^- = \gamma_m^+ = \Gamma_m/N$ when $N > 2$. In fact, as the spectral density of the reservoir is invariant over translation in frequency space, we obtain from Eq. (15) and definition $\Gamma_n \equiv V_{nk}^2(\omega_0)\sigma_n^2(\omega_0)$, the same damping rate as in the weak coupling regime, $\gamma_n(\Omega_m) = \Gamma_n/N$. Thus, for a Markovian white noise reservoir and $N > 2$, the strong coupling between the oscillators does not affect the decoherence time of any joint state of the system, either an eigenstate of normal mode Ω_1 or Ω_ℓ. The system-reservoir couplings around Ω_m are represented by shaded regions in Fig. 3(a).

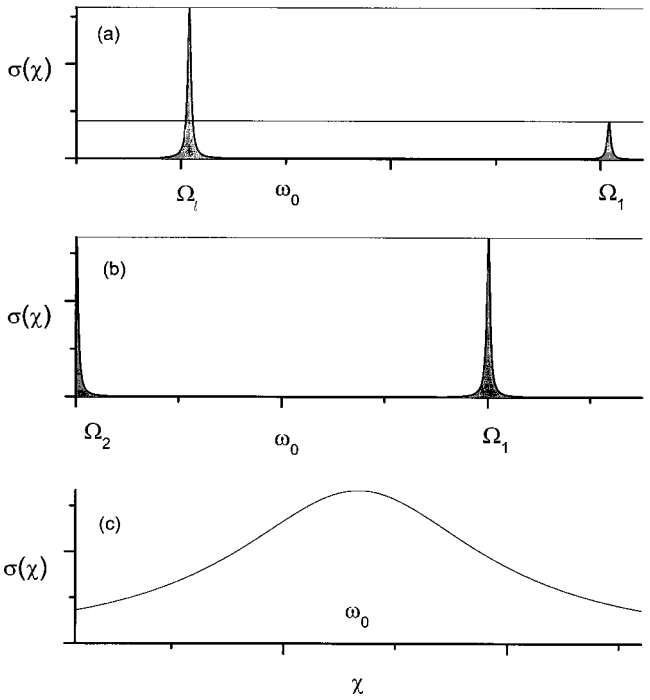

FIG. 3. Spectral density of the reservoir $\sigma_m(\chi)$ for (a) Markovian white noise, and (b) a Lorentzian spectral density. The system-reservoir couplings around the normal modes Ω_1 and Ω_ℓ are represented by the shaded regions.

For the particular case $N=2$ and $\lambda = 2\omega_0$, where $\Omega_2|_{\min} \approx 0$, as discussed above, we get from Eqs. (14a) and (14b) the result $\gamma_m^- = \gamma_m^+/2 = \Gamma_m/4$. As shown in Fig. 3(b), in this case the system-reservoir coupling around $\Omega_2|_{\min} \approx 0$ is half that around frequency Ω_1. Therefore, the strong coupling between the oscillators delays the decoherence time of a joint state which is an eigenstate of normal mode Ω_2. Next, we analyze two cases of non-Markovian colored noise, still assuming that V_m, σ_m, and N_m are functions that vary slowly around the frequency Ω_m, as discussed above.

B. A Lorentzian spectral density and a Bosonic reservoir

Let us consider a Lorentzian spectral density of the reservoir which is considerably smaller than that around ω_0 for the low- ($\chi \ll \omega_0$) and high-frequency ($\chi \gg \omega_0$) domains, as

shown by the solid line in Fig. 3(c). For such a reservoir and $N \gg 1$, both effective frequencies Ω_1 and Ω_ℓ shift to regions around the value $N^2\omega_0$, and consequently $\gamma_m^{\pm} < \Gamma_m/N$. In fact, considering $\sigma_m(\Omega_1) = \epsilon^+ \sigma_m(\omega_0)$ and $\sigma_m(\Omega_\ell) = \epsilon^- \sigma_m(\omega_0)$, where $\epsilon^{\pm} < 1$, we obtain from Eq. (15) the result $\gamma_m^{\pm} = \epsilon^{\pm}\Gamma_m/N$. Therefore, the engineering of such a spectral density would result in a damping function, $\gamma_m(\Omega_m)$, arising from both terms on the right hand side of Eq. (22) (i.e., $\varkappa\sigma_\ell^2/[(\chi - \Omega_{1,\ell})^2 + \varkappa^2] \approx 0$), neither of which would contribute significantly to the relaxation process.

In view of the difficulty of obtaining a Lorentzian spectral density such that $\sigma_m(\Omega_m) = \epsilon\sigma_m(\omega_0)$, we turn to a more realistic case of a Bosonic reservoir whose spectral density is given by the Bose–Einstein distribution function. For such a reservoir, as the cosmic background radiation demanded in Refs. [24,25] to explain the quantum to classical transition, the spectral density is described by the average thermal photon number $\langle n \rangle_\omega = 1/[\exp(\hbar\omega/k_B T) - 1]$, where k_B is the Boltzmann constant. In this case we also get the result $\gamma_m^{\pm} < \Gamma_m/N$, for $N \gg 1$, as in the Lorentzian spectral density considered above.

V. THE FOKKER–PLANCK EQUATION

Using the standard procedures, we derive a *c*-number version of the master equation (17) for the Glauber *P*-function:

$$\frac{d}{dt}P(\{\eta_n\},t) = \sum_m \left(\Pi_m + C_m(\{\eta_n\}) \frac{\partial}{\partial\,\eta_m} + \sum_n D_{mn} \frac{\partial^2}{\partial\,\eta_m\,\partial\,\eta_n^*} + \text{c.c.} \right) P(\{\eta_n\},t), \tag{23}$$

where the function $C_m(\{\eta_n\})$ and the matrix elements D_{mn} satisfy

$$C_m(\{\eta_n\}) = A_m \eta_m + B_m \sum_{n(n\neq m)} \eta_n, \tag{24a}$$

$$D_{mm} = \tfrac{1}{2}[\gamma_m^+ \mathrm{N}_m^+ + (N-1)\gamma_m^- \mathrm{N}_m^-], \tag{24b}$$

$$D_{mn} = \tfrac{1}{4}(\gamma_m^+ \mathrm{N}_m^+ + \gamma_n^+ \mathrm{N}_n^+ - \gamma_m^- \mathrm{N}_m^- - \gamma_n^- \mathrm{N}_n^-), \tag{24c}$$

while the parameters A_m and B_m are given by

$$A_m = \tfrac{1}{2}[\gamma_m^+ + (N-1)\gamma_m^-] + i\tilde{\omega}_0, \tag{25a}$$

$$B_m = \tfrac{1}{2}(\gamma_m^+ - \gamma_m^-) + i\lambda, \tag{25b}$$

with $\Pi_m = \mathrm{Re}(A_m)$.

Considering the reservoirs to be at absolute zero, the Fokker–Planck (FP) equation (23) reduces to a simple drift equation

$$\frac{d}{dt}P(\{\eta_n\},t) = \sum_m \left(\Pi_m + C_m(\{\eta_n\}) \frac{\partial}{\partial\,\eta_m} + \text{c.c.} \right) P(\{\eta_n\},t). \tag{26}$$

With the transformation $P(\{\eta_n\},t) = \tilde{P}(\{\eta_n\},t)\exp(2\Sigma_m\,\Pi_m t)$, and assuming a solution of the drift equation of the form $\tilde{P}(\{\eta_n\},t) = \tilde{P}(\{\eta_n(t)\})$, we obtain

$$\frac{d\tilde{P}}{dt} = \sum_m \left(\frac{d\eta_m}{dt}\frac{\partial\,\tilde{P}}{\partial\,\eta_m} + \text{c.c.} \right) = \sum_m \left(C_m(\{\eta_n\}) \frac{\partial\,\tilde{P}}{\partial\,\eta_m} + \text{c.c.} \right). \tag{27}$$

Therefore, we have to solve the system of coupled equations

$$\frac{d\eta_m}{dt} = A_m \eta_m + B_m \sum_{n(n\neq m)} \eta_n, \tag{28}$$

and this is accomplished by assuming that $\Gamma_\ell = \Gamma_2 \neq \Gamma_1$ (i.e., $\gamma_\ell^{\pm} = \gamma_2^{\pm} \neq \gamma_1^{\pm}$), so that the parameters in Eqs. (25a) and (25b), for $m \neq 1$, simplify to

$$A_\ell = A_2 = \tfrac{1}{2}[\gamma_2^+ + \gamma_2^-(N-1)] + i\tilde{\omega}_0, \tag{29a}$$

$$B_\ell = B_2 = \tfrac{1}{2}(\gamma_2^+ - \gamma_2^-) + i\lambda. \tag{29b}$$

Up to order $\mathcal{O}(\gamma/\lambda)$, the solution of Eq. (28) is given by $\eta_m(t) = e^{\Lambda t}\Sigma_n\, \chi_{mn}(t)\,\eta_n^0$, where $\eta_n^0 = \eta_m(t=0)$,

$$\Lambda = [\gamma_1^+ + \gamma_2^- + (N-1)(\gamma_1^- + \gamma_2^+)]/4 + i\left[\tilde{\omega}_0 + \frac{(N-2)}{2}\lambda \right], \tag{30}$$

and

$$\chi_{11}(t) = \left(f_1(t) + \frac{2\Delta}{N\lambda} f_2(t) \right) g_1(t) - \frac{N-2}{N} f_1(t) g_2(t) + i\left[\left(f_2(t) - \frac{2\Delta}{N\lambda} f_1(t) \right) g_2(t) - \frac{N-2}{N} f_2(t) g_1(t) \right], \tag{31a}$$

$$\chi_{1\ell}(t) = \frac{2}{N}\left[\left(f_1(t) g_2(t) + \frac{\Theta_1}{\lambda} f_2(t) g_1(t) \right) + i\left(f_2(t) g_1(t) - \frac{\Theta_1}{\lambda} f_1(t) g_2(t) \right) \right], \tag{31b}$$

$$\chi_{\ell 1}(t) = \frac{2}{N}\left[\left(f_1(t) g_2(t) + \frac{\Theta_2}{\lambda} f_2(t) g_1(t) \right) + i\left(f_2(t) g_1(t) - \frac{\Theta_2}{\lambda} f_1(t) g_2(t) \right) \right], \tag{31c}$$

$$\chi_{\ell\ell'}(t) = \frac{1}{N-1}\left\{ \left(f_1(t) - \frac{2\Delta}{N\lambda} f_2(t) \right) g_1(t) + \frac{N-2}{N} f_1(t) g_2(t) + i\left[\left(f_2(t) + \frac{2\Delta}{N\lambda} f_1(t) \right) g_2(t) + \frac{N-2}{N} f_2(t) g_1(t) \right] \right\} + \frac{(N-1)\delta_{\ell\ell'} - 1}{N-1} \exp\left\{ \left[N\frac{\gamma_2^-}{2} - \Lambda + i(\tilde{\omega}_0 - \lambda) \right] t \right\}. \tag{31d}$$

The time-dependent functions appearing in Eqs. (31a)–(31c) are given by

$$f_1(t) = \cos(N\lambda t/2), \quad f_2(t) = \sin(N\lambda t/2), \tag{32a}$$

$$g_1(t)=\cosh(\Phi t),\quad g_2(t)=\sinh(\Phi t), \tag{32b}$$

the coefficient argument Φ and the parameters $\Theta_{1,2}$ and Δ satisfying

$$\Phi=[\gamma_1^+-\gamma_2^--(N-1)(\gamma_1^--\gamma_2^+)]/4, \tag{33a}$$

$$\Theta\binom{1}{2}=[\gamma_2^{\mp}-\gamma_1^{\mp}+(N-1)(\gamma_1^{\pm}-\gamma_2^{\pm})]/2N, \tag{33b}$$

$$\Delta=(N-1)(\gamma_1^+-\gamma_2^++\gamma_1^--\gamma_2^-)/2N. \tag{33c}$$

Finally, the solution of the FP equation (26) can be written

$$P(\{\eta_n\},t)=\exp\{2[\Pi_1+(N-1)\Pi_2]t\}P(\{\eta_n\},t=0)\big|_{\eta_n\to\eta_n(t)}. \tag{34}$$

VI. THE DENSITY OPERATOR

Next, with the above assumption that $\gamma_\ell^{\pm}=\gamma_2^{\pm}\neq\gamma_1^{\pm}$, we obtain the density operator $\rho_{1,\ldots,N}(t)$ supposing that the N oscillators are prepared in a superposition of coherent states of the form

$$\begin{aligned}|\Psi_{1,\ldots,N}\rangle&=\mathcal{N}(e^{i\delta_1}|\{\beta_m^1\}\rangle+e^{i\delta_2}|\{\beta_m^2\}\rangle+\cdots+e^{i\delta_J}|\{\beta_m^J\}\rangle)\\&\equiv\mathcal{N}\sum_{p=1}^{J}e^{i\delta_p}|\{\beta_m^p\}\rangle,\end{aligned} \tag{35}$$

where $\mathcal{N}$ stands for the normalization factor, δ_p indicates a phase associated to each state in the superposition, and the subscripts (superscripts) refer to the N oscillators (J distinct states in the superposition). The density operator for the state (35) is given by

$$\begin{aligned}\rho_{1,\ldots,N}(t)&=\int P(\{\eta_n\},t)|\{\eta_n\}\rangle\langle\{\eta_n\}|d^2\{\eta_n\}\\&=\mathcal{N}^2\sum_{p,q=1}^{J}e^{\phi_{pq}+i(\delta_p+\delta_q)}\prod_m\langle\beta_m^q|\beta_m^p\rangle^{1-\Upsilon_{mm}}|\xi_m^p\rangle\langle\xi_m^q|,\end{aligned} \tag{36}$$

where (henceforth $p,q=1,2,\ldots,J$)

$$\phi_{pq}=\frac{1}{2}\sum_{m,n(m\neq n)}[\beta_m^p(\beta_n^{*p}-\beta_n^{*q})-\beta_n^{q*}(\beta_m^p-\beta_m^q)]\Upsilon_{nm}. \tag{37}$$

The evolved states of the oscillators satisfy

$$\xi_m^p(t)=\sum_n\mu_{mn}(t)\beta_n^p, \tag{38}$$

and

$$\Upsilon_{mn}(t)=\sum_{n'}\mu_{n'm}^*(t)\mu_{n'n}(t), \tag{39a}$$

$$\mu_{mn}(t)=e^{-\Lambda t}\chi_{mn}(-t). \tag{39b}$$

The reduced density operator for the mth oscillator, obtained by eliminating the degrees of freedom of all the oscillators but m ($\rho_m(t)=\mathrm{Tr}_{n\neq m}\rho_{1,\ldots,N}$), is given by

$$\rho_m(t)=\mathcal{N}^2\sum_{p,q=1}^{J}e^{\theta_m^{pq}(t)+i(\delta_p+\delta_q)}\left(\prod_n\langle\beta_n^q|\beta_n^p\rangle^{1-|\mu_{mn}(t)|^2}\right)|\xi_m^p\rangle\langle\xi_m^q|, \tag{40}$$

where

$$\begin{aligned}\theta_m^{pq}(t)=\frac{1}{2}\sum_{n,n'(n\neq n')}&[\beta_n^p(\beta_{n'}^{*p}-\beta_{n'}^{*q})-\beta_{n'}^{q*}\\&\times(\beta_n^p-\beta_n^q)]\mu_{mn'}^*(t)\mu_{mn}(t).\end{aligned} \tag{41}$$

VII. DECOHERENCE TIMES

Next, we estimate the decoherence times for some particular states of the network considering two cases: (*i*) all the oscillators in the network having the same damping factor, so that $\Gamma_m=\Gamma$, and (*ii*) oscillator 1 having damping factor Γ_1 and all the other oscillators in the network damping factor $\Gamma_\ell=\Gamma_2$.

(i) Starting with $\Gamma_m=\Gamma$, we estimate the decoherence time for the superposition states which are particular cases of the state (35):

$$\begin{aligned}|\psi_{1,\ldots,N}\rangle&=\mathcal{N}_{\pm}\Big(\Big|\underbrace{\alpha,\ldots,\alpha}_{R},\underbrace{-\alpha,\ldots,-\alpha}_{S},\underbrace{\eta,\ldots,\eta}_{N-R-S}\Big\rangle\\&\quad\pm\Big|\underbrace{-\alpha,\ldots,-\alpha}_{R},\underbrace{\alpha,\ldots,\alpha}_{S},\underbrace{\eta,\ldots,\eta}_{N-R-S}\Big\rangle\Big)\\|\tilde{\phi}_{1,\ldots,N}\rangle&=\mathcal{N}\Big(\Big|\underbrace{\alpha,\ldots,\alpha}_{S},\underbrace{-\alpha,\ldots,-\alpha}_{S},\underbrace{\eta,\ldots,\eta}_{N-2S}\Big\rangle\\&\quad\pm\Big|\underbrace{-\alpha,\ldots,-\alpha}_{S},\underbrace{\alpha,\ldots,\alpha}_{S},\underbrace{\eta,\ldots,\eta}_{N-S}\Big\rangle\Big)\end{aligned} \tag{42}$$

where $R(S)$ indicates the number of oscillators in the coherent state $\alpha(-\alpha)$ in the first term of the superposition and $-\alpha(\alpha)$ in the second term of the superposition. The remaining $N-R-S$ oscillators are in the coherent state η. We note that, as we are considering a symmetric network where all the oscillators have the same damping rates, the oscillators are indistinguishable. Therefore, swapping the states of any two oscillators m and n, we obtain a state which is completely equivalent to Eq. (42). We also note that when $R=1$ and $S=0$, we obtain from (42) the superposition

$$|\tilde{\psi}_{1,\ldots,N}\rangle=\mathcal{N}_{\pm}(|\alpha\rangle\pm|-\alpha\rangle)_1\otimes|\{\eta_\ell\}\rangle, \tag{43}$$

where a quantum superposition of states ("Schrödinger cat"-like state) is prepared in oscillator 1 while all the remaining oscillators are prepared in the coherent states η.

The density operator of the state $|\psi_{1,\ldots,N}\rangle$ in Eq. (42), derived from Eq. (36), is given by

$$\rho_{1,\ldots,N}(t) = \mathcal{N}^2 \sum_{p,q=1}^{2} (\pm)^{1-\delta_{pq}} \exp\{-2|\alpha|^2[(1-\Upsilon+\tilde{\Upsilon})(R+S) - \tilde{\Upsilon}(R-S)^2](1-\delta_{pq}) + \phi_{pq}\}|\{\xi_m^p\}\rangle\langle\{\xi_m^q\}|, \quad (44)$$

where, from Eqs. (37) and (39a),

$$\phi_{pq} = 2i\tilde{\Upsilon}(N-R-S)\mathrm{Im}\left(\eta \sum_{j=1}^{R+S} \beta_j^{*p}\right), \quad (45a)$$

$$\Upsilon = \Upsilon_{mm} = \frac{1}{N}[e^{-N\gamma^+ t} + (N-1)e^{-N\gamma^- t}], \quad (45b)$$

$$\tilde{\Upsilon} = \Upsilon_{mn(m\neq n)} = \frac{1}{N}(e^{-N\gamma^+ t} - e^{-N\gamma^- t}). \quad (45c)$$

From Eq. (44) the coherence decay of the superposition state (42) is given by

$$\exp\left\{-2|\alpha|\left[(1-e^{-N\gamma^- t})(R+S) - \frac{1}{N}(e^{-N\gamma^+ t} - e^{-N\gamma^- t}) \times (R-S)^2\right]\right\} \quad (46)$$

and thus the decoherence time obeys

$$\tau_{D|\psi_{1,\ldots,N}\rangle} = \frac{1}{2|\alpha|^2[N(R+S)\gamma^- + (R-S)^2(\gamma^+ - \gamma^-)]}. \quad (47)$$

When $R=N(S=0)$ or $S=N(R=0)$, giving the superposition $|\phi_{1,\ldots,N}\rangle = \mathcal{N}(|\alpha_1,\ldots,\alpha_N\rangle \pm |-\alpha_1,\ldots,-\alpha_N\rangle)$ (where $\alpha_m=\alpha$), which is an eigenstate of the normal mode $\Omega_1=\tilde{\omega}_0+(N-1)\lambda$, we obtain a result that depends only on the damping rate γ^+:

$$\tau_{D|\phi_{1,\ldots,N}\rangle} = \frac{1}{2N^2|\alpha|^2\gamma^+}. \quad (48)$$

On the other hand, when $R=S$, corresponding to a family of superposition states which are eigenstates of the normal modes $\Omega_\ell=\tilde{\omega}_0-\lambda$,

$$|\tilde{\phi}_{1,\ldots,N}\rangle = \mathcal{N}\left(\left|\underbrace{\alpha,\ldots,\alpha}_{S},\underbrace{-\alpha,\ldots,-\alpha}_{S},\underbrace{\eta,\ldots,\eta}_{N-2S}\right\rangle \pm \left|\underbrace{-\alpha,\ldots,-\alpha}_{S},\underbrace{\alpha,\ldots,\alpha}_{S},\underbrace{\eta,\ldots,\eta}_{N-S}\right\rangle\right)$$

we obtain a result depending only on the damping rate γ^-:

$$\tau_{D|\tilde{\phi}_{1,\ldots,N}\rangle} = \frac{1}{4NS|\alpha|^2\gamma^-}. \quad (49)$$

Evidently, with $S=0$, so that $|\tilde{\phi}_{1,\ldots,N}\rangle = |\eta,\ldots,\eta\rangle$, the coherent states lose excitation without undergoing decoherence, as expected for a reservoir at absolute zero. Finally, when $R=1(0)$ and $S=0(1)$, leading to the state $|\tilde{\psi}_{1,\ldots,N}\rangle$, we obtain the result

$$\tau_{D|\tilde{\psi}_{1,\ldots,N}\rangle} = \frac{1}{2|\alpha|^2}\frac{1}{[\gamma^+ + (N-1)\gamma^-]}, \quad (50)$$

which gives, assuming $N>2$ and Markovian white noise, so that $\gamma^\pm=\Gamma/N$, exactly the expected value for the decoherence time of the superposition state $\mathcal{N}_\pm(|\alpha\rangle \pm |-\alpha\rangle)$ prepared in a single dissipative oscillator: $(2|\alpha|^2\Gamma)^{-1}$.

Next, we analyze the results in Eqs. (48)–(50), considering both of the spectral densities introduced in Sec IV. First, we observe that for $N>2$ the Markovian white noise leads to the same results as the weak-coupling regime, since $\gamma^\pm=\Gamma/N$. However, for the special situation where $N=2$ we obtain different results for the Markovian white noise and the weak-coupling regime, since in the former we get from Eqs. (14a) and (14b) $\gamma^-=\gamma^+/2=\Gamma/4$, whereas in the latter we still get $\gamma^\pm=\Gamma/2$. Therefore, for the general case where $N>2$, we obtain, both for the Markovian white noise (M) and for the weak-coupling regime, where $\gamma^\pm=\Gamma/N$, a decoherence time for the superposition which is an eigenstate of the normal mode Ω_1, given by

$$\tau^M_{D|\phi_{1,\ldots,N}\rangle} = \frac{1}{2N|\alpha|^2\Gamma}, \quad (51)$$

whereas for the eigenstates of the normal modes Ω_ℓ, we obtain

$$\tau^M_{D|\tilde{\phi}_{1,\ldots,N}\rangle} = \frac{1}{4S|\alpha|^2\Gamma}. \quad (52)$$

For the special case where $N=2$, both results in Eqs. (51) and (52) reduce, in the weak-coupling regime, to the value $(4|\alpha|^2\Gamma)^{-1}$ [19] corresponding to the expected decoherence time for the entanglements $|\alpha,\alpha\rangle \pm |-\alpha,-\alpha\rangle$ and $|\alpha,-\alpha\rangle \pm |-\alpha,\alpha\rangle$. In the strong-coupling regime, we still obtain, from Eq. (48), the decoherence time $(4|\alpha|^2\Gamma)^{-1}$ for the eigenstate of the normal mode $\Omega_1: |\alpha,\alpha\rangle \pm |-\alpha,-\alpha\rangle$. However, from Eq. (49) we obtain the value $(2|\alpha|^2\Gamma)^{-1}$, twice as long as in the weak-coupling regime, for the decoherence time of the eigenstate of the normal modes $\Omega_\ell: |\alpha,\alpha\rangle \pm |-\alpha,-\alpha\rangle$. After all, the results in the strong-coupling regime must recover those in the weak-coupling regime when assuming a Markovian white noise reservoir. For the state $|\tilde{\psi}_{1,\ldots,N}\rangle$, we also obtain the expected value of the decoherence time of the superpositions state $\mathcal{N}_\pm(|\alpha\rangle \pm |-\alpha\rangle)_1$:

$$\tau^M_{D|\tilde{\psi}_{1,\ldots,N}\rangle} = \frac{1}{2|\alpha|^2\Gamma}. \quad (53)$$

Considering a Lorentzian spectral density (L) (or a Bosonic reservoir), where $\gamma^\pm \ll \Gamma$, and the case where $N \gg 1$, such that both damping rates assume practically the same value $\gamma^\pm=\epsilon\Gamma/N$ with $\varepsilon<1$, all the values of the decoherence times estimated in Eqs. (51) and (53) are improved, being multiplied by the factor $1/\epsilon$, i.e., $\tau^L_D|_{\gamma^\pm} = \tau^M_D|_{\gamma^\pm}/\epsilon$, and $\tau^L_D = \tau^M_D/\epsilon$. Evidently, the smallness of the factor ϵ depends on the reservoir under consideration.

(ii) We now turn to the case where oscillator 1 has damping factor Γ_1 while all the remaining oscillators of the network have damping factor $\Gamma_2 \ll \Gamma_1$. As we are interested in

improving the decoherence time of a state prepared in oscillator 1, effectively diminishing the damping rate of this oscillator, we assume that $\Gamma_1 \gg \Gamma_2$. In this case we analyze only the state $|\tilde{\psi}_{1,\ldots,N}\rangle$ whose density matrix reads

$$\tilde{\rho}_{1,\ldots,N}(t) = \mathcal{N}_{\pm}^2 \sum_{p,q=1}^{2} (\pm)^{1-\delta_{pq}} \exp[-2|\alpha|^2(1-\Upsilon_{11})(1-\delta_{pq}) + \phi_{pq}] |\{\xi_m^p\}\rangle\langle\{\xi_m^q\}|, \tag{54}$$

where, from Eqs. (37) and (39a), respectively,

$$\phi_{pq} = 2i(N-1)\Upsilon_{1\ell}\mathrm{Im}(\alpha\beta_1^{*p}), \tag{55a}$$

$$\Upsilon_{11} \approx \frac{1}{N}[\exp\{-[\gamma_1^+ + (N-1)\gamma_2^+]t\} + (N-1) \times \exp\{-[\gamma_2^- + (N-1)\gamma_1^-]t\}], \tag{55b}$$

with

$$\Upsilon_{1\ell} \approx \frac{1}{N}[\exp\{-[\gamma_1^+ + (N-1)\gamma_2^+]t\} - \exp\{-[\gamma_2^- + (N-1)\gamma_1^-]t\}]. \tag{56}$$

Therefore, the decoherence time of the state $|\tilde{\psi}_{1,\ldots,N}\rangle$, in the case where all oscillators $\ell = 2,\ldots,N$ have damping rate $\Gamma_2 \neq \Gamma_1$, is given by

$$\tau_D(N) = \frac{1}{2|\alpha|^2} \frac{N}{[\gamma_1^+ + (N-1)(\gamma_2^+ + \gamma_2^-) + (N-1)^2\gamma_1^-]}. \tag{57}$$

In the weak-coupling limit, where $\gamma_m^{\pm} = \Gamma_m/N$, this equation simplifies to

$$\tau_D^{weak}(N) = \frac{1}{2|\alpha|^2} \frac{N^2}{\{[1+(N-1)^2]\Gamma_1 + 2(N-1)\Gamma_2\}}. \tag{58}$$

For the situation where $N \gg 1$, in the weak-coupling limit, the expression (58) leads to the well-known decoherence time of a "Schrödinger cat"-like state $\mathcal{N}_{\pm}(|\alpha\rangle \pm |-\alpha\rangle)$ prepared in a single resonator with a reservoir at absolute zero:

$$\tau_D^{weak}(N \gg 1) = \frac{1}{2|\alpha|^2\Gamma_1}. \tag{59}$$

The maximum value for the decoherence time (58) occurs for the particular case where $N=2$. In this special case where just one other oscillator 2 is coupled to oscillator 1, we obtain a decoherence time which is twice the value in Eq. (59):

$$\tau_D^{weak}(N=2) = \frac{1}{|\alpha|^2\Gamma_1}. \tag{60}$$

In the strong-coupling regime, the decoherence time estimate in Eq. (57) leads exactly to the result (59) assuming $N \gg 1$ and Markovian white noise, where $\gamma_m^{\pm} = \Gamma_m/N$. Moreover, if we assume Markovian white noise with $N=2$ ($\gamma_m^+ = \Gamma_m/2$, $\gamma_m^- = \Gamma_m/4$), we obtain an even better result than that in Eq. (60), given by

$$\tau_D(N=2) = \frac{4}{3}\frac{1}{|\alpha|^2\Gamma_1}. \tag{61}$$

For the Lorenztian spectral density (strong-coupling regime) with $N \gg 1$, so that $\gamma_m^{\pm} = \epsilon\Gamma_m/N$, the time computed in Eq. (59) is improved to the value

$$\tau_D^L(N \gg 1) = \frac{1}{2\epsilon|\alpha|^2\Gamma_1}. \tag{62}$$

We finally stress that the decoherence times for quantum states prepared in a symmetric network with $N>2$ do not depend on the coupling strength λ when considering Markovian-white-noise reservoirs. In fact, for $N>2$ the normal mode $\Omega_\ell = \tilde{\omega}_0 - \lambda$ never reaches zero for Markovian white noise.

VIII. STATE RECURRENCE AND SWAP DYNAMICS

In this section, also considering both cases, where (i) all the oscillators in the network have the same damping factor, $\Gamma_m = \Gamma$, and (ii) all the oscillators but 1 have the same damping factor $\Gamma_\ell = \Gamma_2 \ll \Gamma_1$, we analyze the effect of dissipation on two phenomena: the recurrence of the superposition state $\mathcal{N}_{\pm}(|\alpha\rangle\langle\pm|-\alpha\rangle)_1$ in system 1 and the swapping of this superposition to a particular oscillator of the remaining $N-1$ of the network. This analysis is intended to improve our understanding of the mechanism of coherence loss and, particularly, of the special situation arising in Eqs. (60) and (61) for the decoherence time of the superposition state $\mathcal{N}_{\pm}(|\alpha\rangle \pm |-\alpha\rangle)_1$ prepared in oscillator 1, which is maximized by coupling this oscillator to just one other oscillator 2 with a better quality factor $\Gamma_2 \ll \Gamma_1$. Considering the network prepared in the superposition state (43), $|\tilde{\psi}_{1,\ldots,N}\rangle = \mathcal{N}_{\pm}(|\alpha\rangle \pm |-\alpha\rangle)_1 \otimes |\{\eta_\ell\}\rangle$, and assuming the strong-coupling regime, with the dynamics of the coupled systems governed by the Fokker–Planck equation (34), we calculate the probability that the superposition state $\mathcal{N}_{\pm}(|\alpha\rangle \pm |-\alpha\rangle)_1$, prepared in oscillator 1, returns to this system and the probability of swapping this superposition state to a particular oscillator among the remaining $N-1$, i.e., the probability of the state $\mathcal{N}_{\pm}(|\alpha\rangle \pm |-\alpha\rangle)_1$ being in a given oscillator ℓ. State recurrence and swap dynamics is guaranteed for bipartite coupled systems [26,27]. However, as analyzed below and in Part II of the present work, for a larger composite system both of these dynamics depend on its topology and also on the arrangement of the coupling strengths, such that the collective eigenstates of the system have commensurate frequencies.

We expect that the probability of swapping the state $\mathcal{N}_{\pm}(|\alpha\rangle \pm |-\alpha\rangle)_1$ to a particular oscillator ℓ will never reach unity. In fact, there are $N-1$ oscillators coupled to system 1 and, somehow, the superposition $\mathcal{N}_{\pm}(|\alpha\rangle \pm |-\alpha\rangle)_1$ will be pulverized into the $N-1$ oscillators characterized by the damping rate Γ_2. Evidently, this expectation applies only when all couplings are assumed to have the same strength λ, and in a network where the oscillators couple to each other with different strengths λ_m, it may not be correct. At least in this case (different strengths λ_m) we expect the probability of swapping to reach a value close to unity. When considering the

special case where $N=2$, the probability of a state swap between the two systems, of damping rates Γ_1 and Γ_2, may be unity, as we show below. In this case, the superposition state in oscillator 1 can be protected in oscillator 2 if it has a smaller damping rate Γ_2.

Considering the initial superposition $|\tilde{\psi}_{1,\ldots,N}\rangle$, the reduced density operators for oscillators 1 and ℓ, derived from Eq. (40), are given by

$$\rho_1(t) = \mathcal{N}_{\pm}^2 \sum_{p,q=1}^{2} (\pm)^{1+\delta_{pq}} \exp[-2|\alpha|^2(1-|\mu_{11}|^2)(1-\delta_{pq}) + \theta_1^{pq}] \times |\xi_1^p\rangle\langle\xi_1^q| \tag{63}$$

and

$$\rho_\ell(t) = \mathcal{N}_{\pm}^2 \sum_{p,q=1}^{2} (\pm)^{1+\delta_{pq}} \exp[-2|\alpha|^2(1-|\mu_{\ell 1}|^2)(1-\delta_{pq}) + \theta_\ell^{pq}] \times |\xi_\ell^p\rangle\langle\xi_\ell^q|, \tag{64}$$

where

$$\theta_m^{pq}(t) = 2i\ \mathrm{Im}\left(\eta\beta_1^{*p}\mu_{m1}^*(t)\sum_{\ell}\mu_{m\ell}(t)\right). \tag{65}$$

The probability of recurrence computed from the reduced density operator (63) is given by

$$P_R(t) \equiv \mathrm{Tr}[\rho_1(t)\rho_1(0)] = \sum_{p,q=1}^{2} \mathcal{C}_{pq}^1(t)\langle\xi_1^q|(|\alpha\rangle \pm |-\alpha\rangle)_1(\langle\alpha| \pm \langle-\alpha|)|\xi_1^p\rangle, \tag{66}$$

where the coefficients read

$$\mathcal{C}_{pq}^1(t) = \mathcal{N}_{\pm}^4(\pm)^{1+\delta_{pq}}\exp[-2|\alpha|^2(1-|\mu_{11}|^2)(1-\delta_{pq}) + \theta_1^{pq}]. \tag{67}$$

Analogously to the recurrence probability, we obtain the state-swap probability from the reduced density operator $\rho_\ell(t)$:

$$P_S(t) \equiv \mathrm{Tr}[\rho_\ell(t)\rho_1(0)] = \sum_{p,q=1}^{2} \mathcal{C}_{pq}^\ell(t)\langle\xi_\ell^q|(|\alpha\rangle \pm |-\alpha\rangle)_1(\langle\alpha| \pm \langle-\alpha|)|\xi_\ell^p\rangle, \tag{68}$$

where

$$\mathcal{C}_{pq}^\ell(t) = \mathcal{N}_{\pm}^4(\pm)^{1+\delta_{pq}}\exp[-2|\alpha|^2(1-|\mu_{\ell 1}|^2)(1-\delta_{pq}) + \theta_\ell^{pq}]. \tag{69}$$

In Figs. 4 and 5 we analyze the recurrence and swap probabilities, respectively, for a Markovian white noise. In Fig. 4(a), assuming that all the oscillators have the same damping rate, i.e., $\Gamma_m=\Gamma$, we plot the recurrence probability $P_R(t)$ against the scaled time Γt, taking $\alpha=\eta=1$ as real parameters, $\lambda/\omega_0=2$, and setting the fictitious ratio $\Gamma/\omega_0=1/2$ to show clearly the dissipative dynamics (otherwise, the recurrence frequency would smear the figure). The

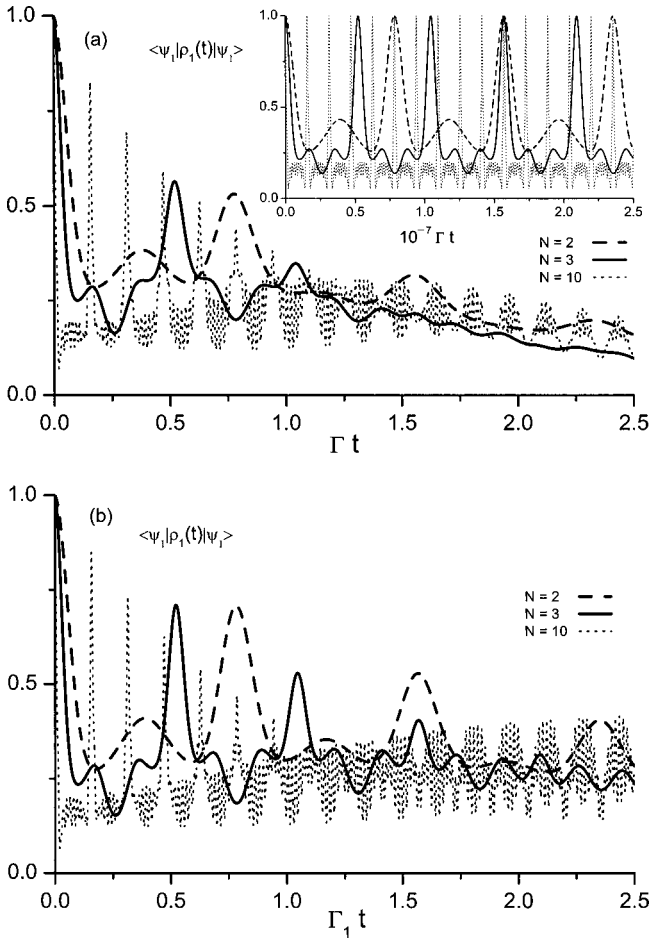

FIG. 4. Recurrence probability $P_R(t)$ plotted against the scaled time (a) Γt, for the case $\Gamma_m=\Gamma$ (setting fictitious ratio $\Gamma/\omega_0=1/2$), and (b) $\Gamma_1 t$, for the case $\Gamma_\ell=\Gamma_2\ll\Gamma_1$ (setting fictitious ratios $\Gamma_1/\omega_0=1/2$ and $\Gamma_2/\omega_0=10^{-2}/2$), assuming Markovian white noise and the factorized state $|\tilde{\psi}_{1,\ldots,N}\rangle=\mathcal{N}_{\pm}(|\alpha\rangle\pm|-\alpha\rangle)_1\otimes|\{\eta_\ell\}\rangle$, with real parameters $\alpha=\eta=1$ and $\lambda/\omega_0=2$. Curves refer to networks with $N=2,3$, and 10 as indicated; inset in (a) shows realistic timescale $\Gamma/\omega_0\ll1$, on which $P_R(t)$ returns to near unity many times before perceptible relaxation occurs.

curves in Fig. 4(a) refer to the values $N=2,3$, and 10, represented by dashed, solid, and dotted lines, respectively. We observe that the recurrence probability $P_R(t)$ decays exponentially due to the dissipative process and that this decay is slower for the case $N=2$ where the coupling strength leads to a normal mode which is shifted to zero and, consequently, $\gamma^-=\gamma^+/2$. For $N>2$, where $\gamma^-=\gamma^+$, we note that the probability $P_R(t)$ decays at the same rate whatever the number of oscillators composing the network, although the oscillations become more frequent as N increases. The recurrence time, which is reduced as the number of oscillators in the network rises, is given by the expression

$$t_R = \frac{2j\pi}{N\lambda}, \quad j=0,1,2,\ldots. \tag{70}$$

Therefore, the recurrence probability $P_R(t)$ exhibits two important features, its frequency and decay rate. It is worth

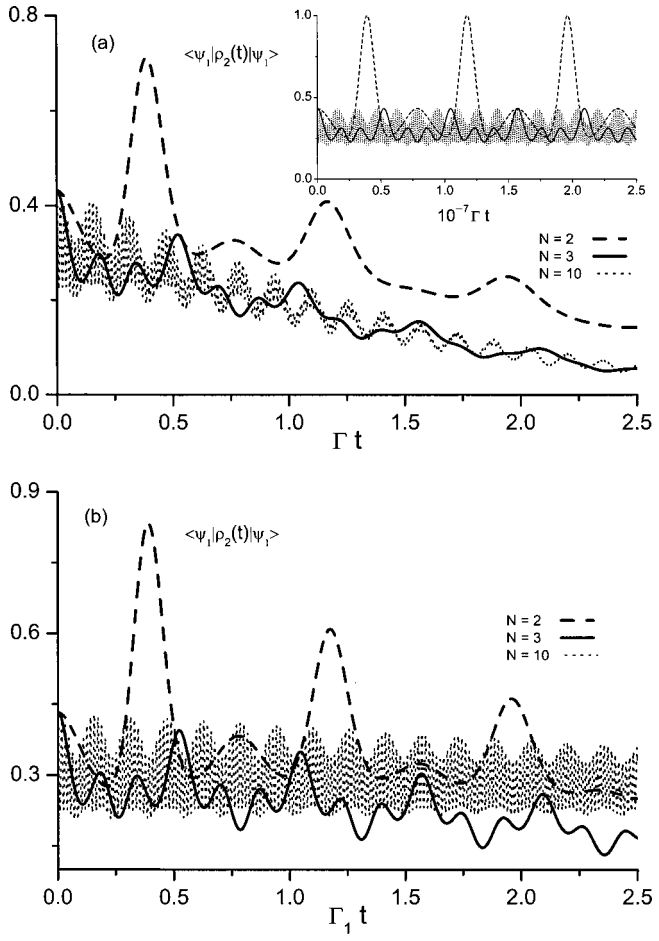

FIG. 5. State-swap probability $P_S(t)$ plotted against the scaled time (a) Γt, for $\Gamma_m=\Gamma$ (setting fictitious $\Gamma/\omega_0=1/2$), and (b) $\Gamma_1 t$, for $\Gamma_\ell=\Gamma_2\ll\Gamma_1$ (setting fictitious $\Gamma_1/\omega_0=1/2$ and $\Gamma_2/\omega_0=10^{-2}/2$), assuming Markovian white noise and the factorized state $|\tilde{\psi}_{1,\ldots,N}\rangle=\mathcal{N}_\pm(|\alpha\rangle\pm|-\alpha\rangle)_1\otimes|\{\eta_\ell\}\rangle$, with real parameters $\alpha=\eta=1$ and $\lambda/\omega_0=2$. Curves refer to networks with 2,3, and 10 oscillators.

stressing that in the weak-coupling regime we obtain a similar behavior for the recurrence probability. Moreover, we point out that on a realistic scale, where $\lambda/\Gamma\approx10^7$ [see the inset in Fig. 4(a)], the probability $P_R(t)$ returns to near unity many times before the relaxation takes place.

In Fig. 4(b), where it is considered that oscillator 1 has damping factor Γ_1 while all the other oscillators in the network have damping factor $\Gamma_2\ll\Gamma_1$, we again plot the recurrence probability $P_R(t)$, now against the scaled time $\Gamma_1 t$, taking $\alpha=\eta=1$ as real parameters, $\lambda/\omega_0=2$, and setting the fictitious ratios $\Gamma_1/\omega_0=1/2$ and $\Gamma_2/\omega_0=10^{-2}/2$. As in Fig. 4(a), the curves for $N=2,3$, and 10 are dashed, solid, and dotted, respectively. We also observe the features pointed out in Fig. 4(a): the frequency and decay-rate of probability $P_R(t)$. However, for the case $\Gamma_2\ll\Gamma_1$, the decay-rate increases, similarly to the frequency, as N increases. Another difference between Figs. 4(a) and 4(b) is that the decay rate for $\Gamma_2\ll\Gamma_1$ is smaller than that for $\Gamma_1=\Gamma_2$ for all values of N. As the decay rate is smaller, the decoherence time for the case $\Gamma_2\ll\Gamma_1$ is longer, as computed in Eq. (58). The difference between the decoherence times in the two cases is maximized to a factor 2 when $N=2$ and reaches zero when $N\gg1$, as confirmed by the decoherence time in Eq. (58).

In Fig. 5(a), considering the case $\Gamma_m=\Gamma$, we plot the state-swap probability $P_S(t)$ for the same parameters as in Fig. 4(a), again for $N=2$ (dashed line), 3 (solid line), and 10 (dotted line). As expected, for $N=2$ the superposition state prepared in oscillator 1 swaps to oscillator 2 before recurring to its original system, and probability $P_S(t)$ decays from unity, due to the damping process. However, for $N>2$ the state-swap process does not occur, i.e., we do not get a significant value for $P_S(t)$ since the superposition state is pulverized into the $N-1$ oscillators connected to oscillator 1. In fact, the state of the network in the "swap times," assumed to be $t_R/2$, comprehends an entanglement of the whole system of the form

$$\mathcal{N}(|\varrho_1,\{\upsilon_\ell\}\rangle+|\tilde{\varrho}_1,\{\tilde{\upsilon}_\ell\}\rangle), \tag{71}$$

where, apart from an irrelevant phase factor, $\varrho_1=[(N-2)(\alpha-2\eta)-2\eta]/N$, $\tilde{\varrho}_1=[(N-2)(\alpha+2\eta)+2\eta]/N$, $\upsilon_\ell=\upsilon=[(N-2)\times(\eta-\alpha)+N\alpha]/N$, and $\tilde{\upsilon}_\ell=\tilde{\upsilon}=[(N-2)(\eta+\alpha)+N\alpha]/N$. The state in Eq. (71), which shows how the "Schrödinger cat"-like state is pulverized into the $\ell=N-1$ oscillators in the network, is obtained considering the initial state $|\tilde{\psi}_{1,\ldots,N}\rangle$ and substituting the "swap times" $t_R/2$ into Eq. (38). We refer to swap times with inverted commas, assumed to be $t_R/2$, for the case $N>2$ where the superposition $\mathcal{N}_\pm(|\alpha\rangle\pm|-\alpha\rangle)_1$ does not swap to the remaining $N-1$ oscillators composing the network with a significant probability.

In Fig. 5(b) we plot the state-swap probability $P_S(t)$ for the case $\Gamma_2\ll\Gamma_1$, assuming the same parameters as in Fig. 4(b). As in Fig. 5(a), the curves for $N=2$, 3,and 10, are dashed, solid, and dotted, respectively. Again, the superposition state $\mathcal{N}_\pm(|\alpha\rangle\pm|-\alpha\rangle)_1$ swaps to oscillator 2 only for $N=2$. However, as we saw when comparing function $P_R(t)$ in Figs. 4(a) and 4(b), the decay rate for the superposition state $\mathcal{N}_\pm(|\alpha\rangle\pm|-\alpha\rangle)_1$ becomes smaller than in the case $\Gamma_1=\Gamma_2$.

IX. ENTROPY EXCESS

In this section, considering again the state $|\tilde{\psi}_{1,\ldots,N}\rangle=\mathcal{N}_\pm(|\alpha\rangle\pm|-\alpha\rangle)_1\otimes|\{\eta_\ell\}\rangle$ and both cases $\Gamma_1=\Gamma_2$ and $\Gamma_2\ll\Gamma_1$, we analyze the linear entropies for the joint state, the reduced state of oscillator 1, and the reduced state of all the remaining $N-1$ oscillators. These functions, computed from Eqs. (54) and (63), in the strong-coupling regime, are given, respectively, by

$$\mathcal{S}_{1,\ldots,N}(t)=1-\mathrm{Tr}_{1,\ldots,N}\tilde{\rho}^2_{1,\ldots,N}(t), \tag{72a}$$

$$\mathcal{S}_1(t)=1-\mathrm{Tr}_1\rho_1^2(t), \tag{72b}$$

$$\mathcal{S}_{2,\ldots,N}(t)=1-\mathrm{Tr}_{2,\ldots,N}[\mathrm{Tr}_1\tilde{\rho}_{1,\ldots,N}(t)]^2. \tag{72c}$$

In order to analyze the evolution of the correlation between the reduced states of oscillator 1 and all the remaining $N-1$ oscillators, we also analyze in this section the excess entropy, here defined as

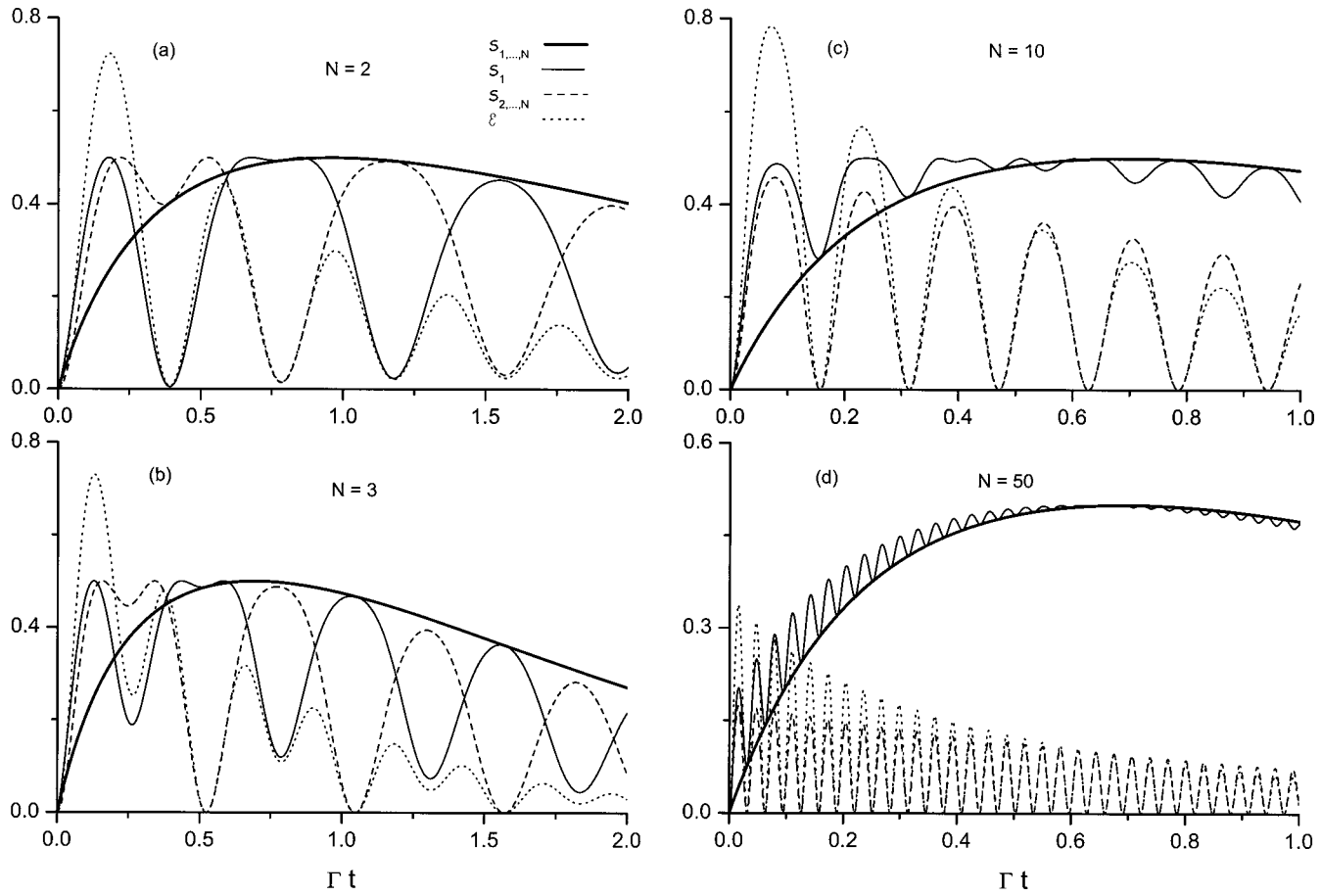

FIG. 6. Linear entropies $\mathcal{S}_{1,\ldots,N}(t)$ (thick solid line), $\mathcal{S}_1(t)$ (solid line), $\mathcal{S}_{2,\ldots,N}(t)$ (dashed line), and excess entropy $\mathcal{E}$ (dotted line) plotted against Γt, for $\Gamma_1=\Gamma_2=\Gamma$ (setting $\lambda/\Gamma=4$), assuming Markovian white noise and the factorized state $|\tilde{\psi}_{1,\ldots,N}\rangle=\mathcal{N}_{\pm}(|\alpha\rangle\pm|-\alpha\rangle)_1\otimes|\{\eta_\ell\}\rangle$, with real parameters $\alpha=\eta=1$. Networks with (a) $N=2$, (b) $N=3$, (c) $N=10$, and (d) $N=50$.

$$\mathcal{E}\equiv\mathcal{S}_1+\mathcal{S}_{2,\ldots,N}-\mathcal{S}_{1,\ldots,N}. \tag{73}$$

In Figs. 6 and 7 we plot the quantities in Eqs. (72a)–(72c) and (73), against the scaled times Γt and $\Gamma_1 t$, considering the cases $\Gamma_1=\Gamma_2=\Gamma$ and $\Gamma_2\ll\Gamma_1$, respectively, and Markovian white noise. We set the ratio $\lambda/\Gamma=4$ in Fig. 6 and, in Fig. 7, we assume $\Gamma_1/\Gamma_2=10^2$ and $\lambda/\Gamma_1=4$. As explained above, these fictitious ratios were chosen to give a clearer picture of the dissipative dynamics. In both figures we take $\alpha=\eta=1$ as real parameters and networks with $N=2$, 3, 10, and 50.

In Figs. 6(a) and 7(a) we considered the case $N=2$, exhaustively analyzed in Ref. [19]. In these figures, the thick solid line representing the linear entropy of the joint state $\mathcal{S}_{1,2}$ starts from zero, goes to a maximum due to the decoherence process (or the entanglement between the subsystems), and then returns to zero, since in the asymptotic limit all oscillators reach the vacuum. Meanwhile, the linear entropies of the reduced states $\mathcal{S}_1$ and $\mathcal{S}_2$, represented by solid and dashed lines, respectively, oscillate between 0 and 0.5. The function $\mathcal{S}_1(\mathcal{S}_2)$ reaches its minima when oscillator 1 (oscillator 2) assumes (recovers) the state $|-\eta\rangle_1(|\eta\rangle_2)$, as can be computed from Eq. (38) [19]. At the same time, $\mathcal{S}_2(\mathcal{S}_1)$ touches the thick solid line representing $\mathcal{S}_{1,2}$, from above, indicating that the superposition $\mathcal{N}_{\pm}(|\alpha\rangle\pm|-\alpha\rangle)_1$ has swapped (recurred) to oscillator 2 (1) on its way to decoherence. We conclude that it is exactly the state $\mathcal{N}_{\pm}(|\alpha\rangle\pm|-\alpha\rangle)_1$ which recurs (swaps) to oscillator 1 (2) in Figs. 4 and 5, which show clearly (considering realistic parameters) that this superposition does recur and swap to oscillator 1 (2), respectively. Therefore, as the superposition $\mathcal{N}_{\pm}(|\alpha\rangle\pm|-\alpha\rangle)_1$, prepared in oscillator 1, swaps to oscillator 2 and is subsequently recovered by oscillator 1, the coherent state $|\eta\rangle_2$, prepared in oscillator 2, does recur to this system, but it is not swapped to oscillator 1 (as emphasized in Ref. [19]) which, instead, acquires the state $|-\eta\rangle_1$.

We also observe in Figs. 6(a) and 7(a) that the maximal correlations between oscillators 1 and 2 occur at the points where the curves $\mathcal{S}_1$ and $\mathcal{S}_2$ cross, as illustrated by the dotted line representing the excess entropy $\mathcal{E}$. When the linear entropy $\mathcal{S}_1$ or $\mathcal{S}_2$ touches the curve of $\mathcal{S}_{1,2}$, i.e., when the superposition state $\mathcal{N}_{\pm}(|\alpha\rangle\pm|-\alpha\rangle)_1$ recurs to oscillator 1 or swaps to oscillator 2, both the excess entropy and the correlation between the oscillators reach their minima. It is worth noting that, as time goes on, the oscillators do not get completely disentangled since the excess entropy does not reach zero. As analyzed in Ref. [19], where only the case $N=2$ was considered, the minima of the excess entropy $\mathcal{E}$ move away from zero due to the development of an inevitable background correlation between the oscillators which thus become entangled as the linear entropy of the joint state $\mathcal{S}_{1,2}$

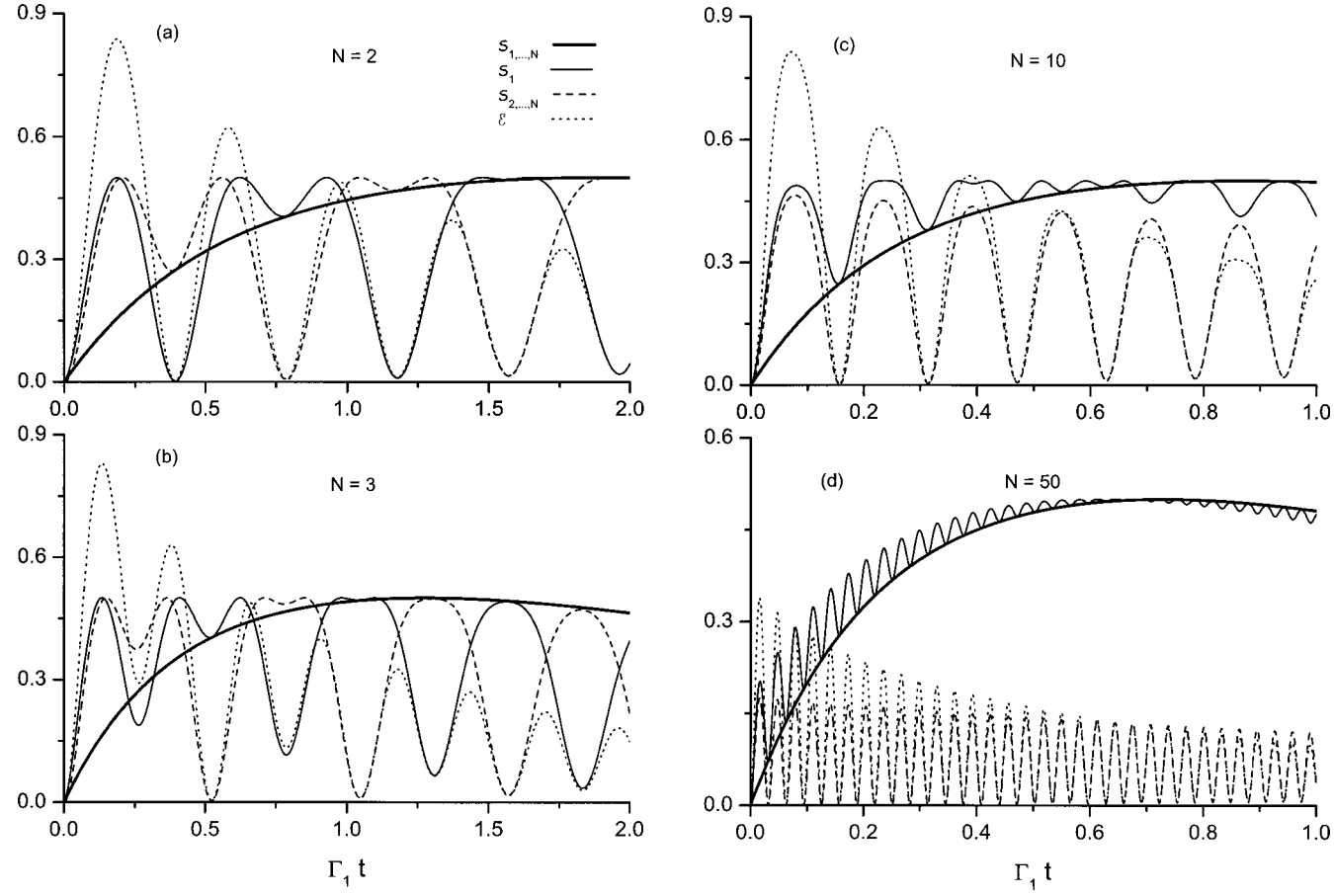

FIG. 7. Linear entropies $\mathcal{S}_{1,\ldots,N}(t)$ (thick solid line), $\mathcal{S}_1(t)$ (solid line), $\mathcal{S}_{2,\ldots,N}(t)$ (dashed line), and excess entropy $\mathcal{E}$ (dotted line) plotted against $\Gamma_1 t$, for $\Gamma_2 \ll \Gamma_1$ (setting $\Gamma_1/\Gamma_2 = 10^2$ and $\lambda/\Gamma_1 = 4$), assuming Markovian white noise and the factorized state $|\tilde{\psi}_{1,\ldots,N}\rangle = \mathcal{N}_{\pm}(|\alpha\rangle \pm |-\alpha\rangle)_1 \otimes |\{\eta_\ell\}\rangle$, with real parameters $\alpha = \eta = 1$. Networks with (a) 2, (b) 3, (c) 10, and (d) 50 oscillators.

goes to a maximum. Evidently, the minima of the excess entropy $\mathcal{E}$ return to zero, as does the linear entropy of the joint state $\mathcal{S}_{1,2}$, as the whole system approaches the vacuum. This background correlation arises from two different processes: (*i*) the cross-decay channels ($\mathcal{L}_{mn}\rho_{1,\ldots,N}(t)$) which link together the individual Liouville operators $\mathcal{L}_m\rho_{1,\ldots,N}(t)$ and (*ii*) the usual decay channels ($\mathcal{L}_m\rho_{1,\ldots,N}(t)$), when the decay rates Γ_n are different from each other. For equal decay rates, the individual decay channels do not contribute to the development of the background correlation.

For the case $\Gamma_1 = \Gamma_2 = \Gamma$, assuming Markovian white noise, the development of this background correlation occurs only for $N = 2$, since the cross-decay channel $\mathcal{L}_{12}\rho_{12}$ is null for $N > 2$ (and the decay rates are equal). In fact, for $N = 2$ we have in the Markovian white noise $\gamma^- = \gamma^+/2 = \Gamma/4$, while for $N > 2$ we have $\gamma^- = \gamma^+ = \Gamma/N$. Due to this background correlation coming from the cross-decay channel $\mathcal{L}_{12}\rho_{12}$, oscillator 1 (2) never recovers (assumes) exactly the state $\mathcal{N}_{\pm}(|\alpha\rangle \pm |-\alpha\rangle)_1$: the probability of the state $\mathcal{N}_{\pm}(|\alpha\rangle \pm |-\alpha\rangle)_1$ recurring (swapping) to oscillator 1 (2) decreases as the linear entropy of the joint state increases, reaches a maximum and returns to zero. Similarly, oscillator 1 (2) never assumes (recovers) exactly the state $|-\eta\rangle_1(|\eta\rangle_2)$.

In Figs. 6(b) and 7(b) we consider $N = 3$. In this case, as discussed above and indicated in figures, we lose the swap of the superposition state $\mathcal{N}_{\pm}(|\alpha\rangle \pm |-\alpha\rangle)_1$ to system "2+3" (when assuming the same coupling strength between all the oscillators). As a matter of fact, to which oscillator, 2 or 3, would this superposition swap into? As long as we assume the same coupling strength between the oscillators, the superposition must be shared between oscillators 2 and 3. It will not be found in system "2+3" with a significant probability that could be interpreted as a swap process. Therefore, there is no state swap between the reduced systems 1 and "2+3;" the functions $\mathcal{S}_1$ and $\mathcal{S}_{2,3}$ go through what we may call "local minima," before the recurrence processes, where one of these functions reaches zero and the other touches the curve for $\mathcal{S}_{1,2,3}$. Consequently, the excess entropy $\mathcal{E}$ also goes through "local minima" (where the swap processes were expected to occur), since at these points systems 1 and "2+3" exhibit a significant degree of entanglement. As in Figs. 6(a) and 7(a), the maximal correlations between these reduced systems still occur at the points where the curves $\mathcal{S}_1$ and $\mathcal{S}_{2,3}$ cross, as indicated by the dotted line representing $\mathcal{E}$. The difference between Figs. 6(b) and 7(b) is that in the latter there is the development of a background correlation between the oscillators, as occurs in the case $N = 2$. In fact, for $\Gamma_2 \neq \Gamma_1$, the different decay rates of the individual Liouville operators $\mathcal{L}_m\rho_{1,2,3}(t)$ lead to the development of the background correlation. Note that in the Markovian white noise the cross-decay channels $\Sigma_{m,n=1(m\neq n)}^{3}\,\mathcal{L}_{mn}\rho_{1,2,3}$ are null and

do not contribute to the background correlation. Thus, different decay rates of the individual Liouville operators lead to the development of a background correlation even when the cross-decay channels are null.

While the state-swap processes are lost if $N>2$, the recurrence processes are not: when $\mathcal{S}_1$ touches the thick solid line of $\mathcal{S}_{1,\ldots,N}$, the state $\mathcal{N}_{\pm}(|\alpha\rangle\pm|-\alpha\rangle)_1$ recurs to oscillator 1 on its way to decoherence, as indicated in Figs 6 and 7(b)–7(d) for $N=3,10,50$, respectively. Simultaneously, when $\mathcal{S}_{2,\ldots,N}$ touches zero, the coherent states $|\eta,\ldots,\eta\rangle_{2,\ldots,N}$ recur to system "$2+\cdots+N$". Evidently, for the case $\Gamma_2\ll\Gamma_1$ in Fig. 7, the states recurring to systems "1" and "$2+\cdots+N$" are not exactly the superposition $\mathcal{N}_{\pm}(|\alpha\rangle\pm|-\alpha\rangle)_1$ and the coherent states $|\eta,\cdots,\eta\rangle_{2,\ldots,N}$, respectively, owing to the development of the background correlation. However, even though the systems 1 and "$2+\cdots+N$" do not get completely disentangled at the recurrence times, a *small* network with $\Gamma_2\ll\Gamma_1$ may be considered to protect, in system "$2+\cdots+N$", the superposition state $\mathcal{N}_{\pm}(|\alpha\rangle\pm|-\alpha\rangle)_1$ prepared in oscillator 1. As seen in Eq. (58), in a small network we obtain a decoherence time for the superposition $\mathcal{N}_{\pm}(|\alpha\rangle\pm|-\alpha\rangle)_1$ about twice that derived for a single dissipative oscillator. As the number of oscillators in the network rises, the decoherence time approaches that for a single dissipative oscillator. In fact, the decoherence time computed from Eq. (58), for the case $N=3$ and $\Gamma_2\ll\Gamma_1$, is $\frac{9}{5}$ times the value computed when this superposition is prepared in a single dissipative oscillator. For a network with $N=5$, the decoherence time is about $\frac{3}{2}$ times the value computed for a single dissipative oscillator.

Moreover, it is crucial to note that the background correlation does not affect significantly the fidelity of the recovered superposition $\mathcal{N}_{\pm}(|\alpha\rangle\pm|-\alpha\rangle)_1$ when considering a network where $\Gamma_2\ll\Gamma_1$. In fact, whatever the spectral distribution function, the correlation time arising from the development of the background correlation, estimated as the time when the minima of $\mathcal{E}$ approach 10^{-2}, is given by

$$\tau_C\approx\frac{N}{10|\alpha|\sqrt{N-1}|\gamma_1^+-\gamma_2^-+(N-1)(\gamma_2^+-\gamma_1^-)|}. \quad (74)$$

From Eq. (74) we conclude that for the weak-coupling regime, where $\gamma_\ell^+=\gamma_\ell^-=\Gamma_\ell/N$, and in the case when all the oscillators in the network have the same damping factor, $\Gamma_m=\Gamma$, the background-correlation time goes to infinity, i.e., the entropy $\mathcal{S}_{2,\ldots,N}$ always returns to zero in the recurrence time. For $\Gamma_2\neq\Gamma_1$ and considering the decoherence time τ_D computed in the strong-coupling regime [Eq. (57)], we obtain the ratio τ_C/τ_D

$$\frac{\tau_C}{\tau_D}\approx\frac{|\alpha|[\gamma_1^+ +(N-1)(\gamma_2^+ +\gamma_2^-)+(N-1)^2\gamma_1^-]}{5\sqrt{N-1}|\gamma_1^+-\gamma_2^-+(N-1)(\gamma_2^+-\gamma_1^-)|}. \quad (75)$$

When $\tau_C/\tau_D\gtrsim 1$ one can always recover the superposition state $\mathcal{N}_{\pm}(|\alpha\rangle\pm|-\alpha\rangle)$ in oscillator 1, with considerable fidelity, in spite of the background correlation (i.e., the process of entanglement between the oscillators composing the network). Evidently, for $\tau_C/\tau_D\gtrsim 1$ the correlation time becomes greater than the decoherence time, and thus becomes negligible for state protection purposes. For a network with $N>2$ and $\Gamma_2\ll\Gamma_1$, we obtain from Eq. (75), assuming Markovian white noise, the result

$$\frac{\tau_C}{\tau_D}\approx\frac{|\alpha|[(N-1)^2+1]}{5\sqrt{N-1}(N-2)}. \quad (76)$$

As an example, for $N=5$ we get $\tau_C/\tau_D\approx|\alpha|/2$ so that, starting with a coherent state $|\alpha|\gtrsim 2$, we can recover the superposition state $\mathcal{N}_{\pm}(|\alpha\rangle\pm|-\alpha\rangle)_1$ protected in system "$2+\cdots+5$" with good fidelity. Evidently, for $N>5$ we get a ratio τ_C/τ_D greater than unity even for $|\alpha|$ smaller than 2. This is an important result since the superposition state $\mathcal{N}_{\pm}(|\alpha\rangle\pm|-\alpha\rangle)_1$, prepared in oscillator 1, can be protected against decoherence in system "$2+\cdots+N$", when $\Gamma_2\ll\Gamma_1$, and eventually recovered in oscillator 1. However, we stress again (in the context of Markovian white noise) that with $N>2$ the state protection is not as efficient as when $N=2$. The mechanism of state protection by adopting $\Gamma_2\ll\Gamma_1$ might be employed in cavity quantum electrodynamics, where a superposition state $\mathcal{N}_{\pm}(|\alpha\rangle\pm|-\alpha\rangle)_1$ could be prepared in an open "bad-quality" cavity, protected against decoherence in a system of closed "good-quality" cavities and recovered in the open cavity, say, for atom-field interaction purposes.

Considering a network with the same damping factor, $\Gamma_m=\Gamma$, in the strong coupling regime, we obtain from Eq. (75) the expression

$$\frac{\tau_C}{\tau_D}\approx\frac{|\alpha|[\gamma^+ +(N-1)\gamma^-]}{5\sqrt{N-1}|\gamma^+-\gamma^-|}. \quad (77)$$

For $N>2$ and assuming Markovian white noise, we obtain $\tau_C/\tau_D\to\infty$ as expected from Figs. 6(b)–6(d). For $N=2$ we get $\tau_C/\tau_D=3|\alpha|/5$ so that, for $|\alpha|\gtrsim 2$, we obtain $\tau_C/\tau_D\gtrsim 1$.

We finally note that, when preparing a "Schrödinger cat"-like state in oscillator 1, the network works as part of reservoir R_1 as indicated in Figs. 6(d) and 7(d). In fact, these figures indicate that when $N>>1$ the evolution of the superposition state $\mathcal{N}_{\pm}(|\alpha\rangle\pm|-\alpha\rangle)$ prepared in oscillator 1 does not depend on the network. The linear entropy for the joint state, $\mathcal{S}_{1,\ldots,N}(t)$, coincides with that for the reduced state of oscillator 1, $\mathcal{S}_1(t)$, throughout the evolution.

X. CONCLUSION

In this paper we have analyzed the coherence dynamics and the decoherence process of quantum states in a network composed of N coupled dissipative oscillators. Assuming all oscillators to have the same natural frequency ω_0 and all couplings the same strength λ, we considered both weak and strong coupling regimes between the oscillators (see below). Moreover, we considered a symmetric network where each oscillator interacts with all others.

When all oscillators have the same natural frequency ω_0 and interact with each other with the same strength λ, we observe that the network displays only two different normal modes, Ω_1 and Ω_ℓ, as defined in Eqs. 6(a) and 6(b), respectively. A central result is that in the strong-coupling regime the damping rate for each oscillator, Γ_m (computed from a function centered around the normal mode ω_0), splits into

two different values γ_m^+ and γ_m^- (computed from functions centered around the normal modes, Ω_1 and Ω_ℓ, respectively). In the weak-coupling regime there is no split of the damping rate, so that $\gamma_m^+ = \gamma_m^- = \Gamma_m/N$, where Γ_m defines the damping constant of a single dissipative oscillator. The split damping constants γ_m^+ and γ_m^-, in the strong-coupling regime, can assume completely different values depending on the spectral density of the reservoirs associated with the oscillators composing the network. Since the magnitude of these damping constants depends on the spectral density around the normal modes, the splitting mechanism can be used to control the decoherence process of quantum states of the network. Therefore, the program of engineering particular spectral densities of the reservoir becomes crucial for controlling the decoherence process of strongly interacting quantum oscillators.

We observe that we have called "strong-coupling regime" the situations where the parameter $\lambda(N-1)$ is large enough to shift the normal modes to regions far away from the natural frequency ω_0. These situations arise on increasing the strength of the coupling between the oscillators and/or the number of oscillators in the network. In this light, we note than in a realistic quantum logic processor, the number of dissipative nodes must always be a concern when analyzing coherence dynamics and estimating decoherence times, since cross-decay channels could occur even with a weak coupling strength.

Another consequence of the strong-coupling regime, related to the splitting of the damping rates, is the appearance of cross-decay channels in the master equation of the network as described in Eqs. (17) and (19). These cross-decay channels link together the individual decay channels described by the Liouville operators $\mathcal{L}_m \rho_{1,\ldots,N}(t)$. As we see in Eq. (19), these cross-decay channels become null when $\gamma_m^+ = \gamma_m^-$, which always occurs in the weak-coupling regime and, for Markovian white noise, also in the strong-coupling regime. The cross-decay channels are responsible for the emergence of a background correlation, i.e., a permanent residual correlation, between the oscillators composing the network. As stressed above, when the cross-decay channels are null, differences between decay rates of individual Liouville operators also lead to the development of a background correlation.

Considering a symmetric network, we have computed the decoherence time for entangled and factorized quantum states of the network in the strong coupling regime. The expression thus computed can easily be converted to the weak-coupling regime. In particular, we computed the decoherence time for the factorized state $|\tilde{\psi}_{1,\ldots,N}\rangle = \mathcal{N}_\pm(|\alpha\rangle \pm |-\alpha\rangle)_1 \otimes |\{\eta_\ell\}\rangle$, where a Schrödinger-cat-like state is prepared in oscillator 1 while all the remaining $N-1$ oscillators are prepared in the coherent states η. We assumed that oscillator 1 has damping factor Γ_1 while all the other $N-1$ oscillators of the network have damping factor $\Gamma_2 \ll \Gamma_1$. We found that the decoherence time of the Schrödinger-cat-like state $\mathcal{N}_\pm(|\alpha\rangle \pm |-\alpha\rangle)_1$, prepared in oscillator 1 of the network, has the maximum value $(|\alpha|^2\Gamma_1)^{-1}$ for $N=2$, when only one other oscillator, with damping rate Γ_2, is coupled to oscillator 1, whose damping rate is Γ_1. On increasing the number N of oscillators in the network, the decoherence time decreases gradually, reaching the well-known value $(2|\alpha|^2\Gamma_1)^{-1}$ [computed for a superposition $\mathcal{N}_\pm(|\alpha\rangle \pm |-\alpha\rangle)_1$ prepared in a single dissipative oscillator] when $N \to \infty$.

To understand this interesting result, we analyzed the (*i*) state recurrence and (*ii*) state swap dynamics, i.e., (*i*) the probability that the superposition state $\mathcal{N}_\pm(|\alpha\rangle \pm |-\alpha\rangle)_1$, prepared in oscillator 1, recurs in this system and (*ii*) the probability of swapping this superposition to a particular oscillator other than oscillator 1 [i.e., the probability of the state $\mathcal{N}_\pm(|\alpha\rangle \pm |-\alpha\rangle)_1$ being in a given oscillator of the remaining $N-1$]. We found that the state-swap process occurs only when $N=2$, so that the superposition $\mathcal{N}_\pm(|\alpha\rangle \pm |-\alpha\rangle)_1$, prepared in oscillator 1, is protected in oscillator 2, which has a smaller damping rate. Otherwise, for $N>2$, the swap process does not occur with a significant probability and the superposition cannot be efficiently protected in the remaining $N-1$ oscillators of the network. In fact, when oscillator 1 is coupled to a system of $\ell > 2$ oscillators, how could the superposition $\mathcal{N}_\pm(|\alpha\rangle \pm |-\alpha\rangle)_1$ swap to the remaining oscillators? This superposition is somehow pulverized into the remaining $N-1$ oscillators of the network, so that it will never be found in one of them with significant probability and, therefore, the state protection will not be as efficient as when $N=2$.

We also analyzed the linear entropies for the joint state, $\mathcal{S}_{1,\ldots,N}$, the reduced state of oscillator 1, $\mathcal{S}_1$, and the reduced state of all the remaining $N-1$ oscillators, $\mathcal{S}_{2,\ldots,N}$, as defined by Eqs. (72a)–(72c). The quantity we call the excess entropy, $\mathcal{E} \equiv \mathcal{S}_1 + \mathcal{S}_{2,\ldots,N} - \mathcal{S}_{1,\ldots,N}$, was also computed. We found that, apart from losing the state-swap process when $N>2$, i.e., the superposition $\mathcal{N}_\pm(|\alpha\rangle \pm |-\alpha\rangle)$ cannot be found in the remaining $N-1$ oscillators with a significant probability, this superposition hardly leaves oscillator 1 when $N \gg 1$. In fact, the frequency of the state-currence process becomes higher as we increase the number N of oscillators composing the network. Here is an interesting aspect of the coherence dynamics in a quantum network: when a superposition state is prepared in a particular dissipative oscillator 1 in a very large symmetric network of N dissipative coupled oscillators, this superposition state decays as if the dissipative oscillator 1 were decoupled from the network. Therefore, in this case the remaining $N-1$ oscillators of the network cannot be distinguished from the reservoir modes of oscillator 1.

ACKNOWLEDGMENTS

We wish to express thanks for the support from the Brazilian agencies FAPESP (under Contract Nos. 99/11859-3, 00/15084-5, and 02/02633-6) and CNPq (Intituto do Milênio de Informação Quântica). We also thank R. M. Serra, C. J. Villas-Bôas, P. S. Pizani, V. V. Dodonov, S. S. Mizrahi, and A. F. R. de Toledo Piza for helpful discussions.

[1] P. Shor, in *Proceedings of the 35th Annual Symposium on the Theory of Computer Science*, edited by. S. Goldwasser (IEEE Computer Society, Los Alamitos, CA, 1994), p. 124; e-print quant-ph/9508027.

[2] J. I. Cirac, P. Zoller, H. J. Kimble, and H. Mabuchi, Phys. Rev. Lett. **78**, 3221 (1997); T. Pellizzari, *ibid.* **79**, 5242 (1997); H. J. Briegel, W. Dür, J. I. Cirac, and P. Zoller, *ibid.* **81**, 5932 (1998); S. J. van Enk, H. J. Kimble, J. I. Cirac, and P. Zoller, Phys. Rev. A **59**, 2659 (1999).

[3] J. I. Cirac and P. Zoller, Phys. Rev. Lett. **74**, 4091 (1995); Q. A. Turchette, C. J. Hood, W. Lange, H. Mabuchi, and H. J. Kimble, *ibid.* **75**, 4710 (1995); I. L. Chuang, L. M. K. Vandersypen, X. Zhou, D. W. Leung, and S. Lloyd, Nature (London) **393**, 143 (1998); B. E. Kane, *ibid.* **393**, 143 (1998); L. M. K. Vandersypen, M. Steffen, G. Breyta, C. S. Yannoni, M. H. Sherwood, and I. L. Chuang, *ibid.* **414**, 883 (2001); **414**, 883 (2001).

[4] C. H. Bennett, Phys. Today **48**, 24 (1995); C. H. Bennett and D. P. Divincenzo, Nature (London) **377**, 389 (1995).

[5] C. H. Bennett, G. Brassard, C. Crépeau, R. Jozsa, A. Peres, and W. K. Wootters, Phys. Rev. Lett. **70**, 1895 (1993).

[6] C. J. Villas-Bôas, N. G. de Almeida, and M. H. Y. Moussa, Phys. Rev. A **60**, 2759 (1999); R. M. Serra, C. J. Villas-Bôas, N. G. de Almeida, and M. H. Y. Moussa, J. Opt. B: Quantum Semiclassical Opt. **4**, 316 (2002).

[7] W. H. Zurek, Phys. Rev. D **24**, 1516 (1981); **26**, 1862 (1982); Phys. Today **44**(10), 36 (1991).

[8] A. O. Caldeira and A. J. Leggett, Ann. Physics **149**, 374 (1983); Physica A **121**, 587 (1983).

[9] S. Haroche, Phys. Today **51**(7), 36 (1998).

[10] P. W. Shor, Phys. Rev. A **52**, R2493 (1995); L. Vaidman, L. Goldenberg, and S. Wiesner, *ibid.* **54**, R1745 (1996); W. H. Zurek and R. Laflamme, *ibid.* **77**, 4683 (1996); A. R. Calderbank, E. M. Rains, P. W. Shor, and N. J. A. Sloane, *ibid.* **78**, 405 (1997).

[11] J. F. Poyatos, J. I. Cirac, and P. Zoller, Phys. Rev. Lett. **77**, 4728 (1996).

[12] C. J. Myatt, B. E. King, Q. A. Turchette, C. A. Sackett, D. Kielpinski, W. M. Itano, C. Monroe, and D. J. Wineland, Nature (London) **403**, 269 (2000).

[13] A. R. R. Carvalho, P. Milman, R. L. de Matos Filho, and L. Davidovich, Phys. Rev. Lett. **86**, 4988 (2001).

[14] N. Lutkenhaus, J. I. Cirac, and P. Zoller, Phys. Rev. A **57**, 548 (1998).

[15] L. M. K. Vandersypen, M. Steffen, G. Breyta, C. S. Yannoni, M. H. Sherwood, and I. L. Chuang, Nature (London) **414**, 883 (2001).

[16] S. G. Mokarzel, A. N. Salgueiro, and M. C. Nemes, Phys. Rev. A **65**, 044101 (2002).

[17] J. M. Raimond, M. Brune, and S. Haroche, Phys. Rev. Lett. **79**, 1964 (1997).

[18] H. Zoubi, M. Orenstien, and A. Ron, Phys. Rev. A **62**, 033801 (2000).

[19] M. A. de Ponte, M. C. de Oliveira, and M. H. Y. Moussa, e-print quant-ph/0309082.

[20] G. Teklemariam, E. M. Fortunato, C. C. Lopez, J. Emerson, Jaun Pablo Paz, T. F. Havel, and D. G. Cory, Phys. Rev. A **67**, 062316 (2003).

[21] G. W. Ford, J. T. Lewis, and R. F. O'Connell, Phys. Rev. A **37**, 4419 (1988); G. W. Ford and R. F. O'Connell, Physica A **37**, 377 (1997).

[22] M. Rosenau da Costa, A. O. Caldeira, S. M. Dutra, and H. Westfahl, Jr., Phys. Rev. A **61**, 022107 (2000).

[23] N. Studart and S. S. Sokolov, in *Two-Dimensional Electron System*, edited by E. Y. Andrei (Kluwer Academic, Dordrecht, Netherlands, 1997).

[24] E. Joos and H. D. Zeh, Z. Phys. B: Condens. Matter **59**, 223 (1985).

[25] M. C. de Oliveira, N. G. Almeida, S. S. Mizrahi, and M. H. Y. Moussa, Phys. Rev. A **62**, 012108 (2000).

[26] P. Bocchieri and A. Loinger, Phys. Rev. **107**, 337 (1957).

[27] M. C. de Oliveira, S. S. Mizrahi, and V. V. Dodonov, J. Opt. B: Quantum Semiclassical Opt. **1**, 610 (1999).